AD_____

Award Number: W81XWH-05-1-0322

TITLE: Roles of Breast Cancer Susceptibility Genes BRCA's in Mammary Epithelial Cell Differentiation

PRINCIPAL INVESTIGATOR: Dr. Saori Furuta

CONTRACTING ORGANIZATION: The University of California
Irvine, CA 92697

REPORT DATE: March 2006

TYPE OF REPORT: Annual Summary

PREPARED FOR: U.S. Army Medical Research and Materiel Command
Fort Detrick, Maryland 21702-5012

REPORT DOCUMENTATION PAGE

Form Approved
OMB No. 0704-0188

1. REPORT DATE *(DD-MM-YYYY)*	**2. REPORT TYPE**	**3. DATES COVERED** *(From - To)*
01-03-2006	Annual Summary	1 MAR 2005 - 28 FEB 2006

4. TITLE AND SUBTITLE
Roles of Breast Cancer Susceptibility Genes BRCA's in Mammary Epithelial Cell Differentiation

5a. CONTRACT NUMBER

5b. GRANT NUMBER
W81XWH-05-1-0322

5c. PROGRAM ELEMENT NUMBER

6. AUTHOR(S)
Dr. Saori Furuta

E-mail: sfuruta@uci.edu

5d. PROJECT NUMBER

5e. TASK NUMBER

5f. WORK UNIT NUMBER

7. PERFORMING ORGANIZATION NAME(S) AND ADDRESS(ES)

The University of California
Irvine, CA 92697

8. PERFORMING ORGANIZATION REPORT NUMBER

9. SPONSORING / MONITORING AGENCY NAME(S) AND ADDRESS(ES)
U.S. Army Medical Research and Materiel Command
Fort Detrick, Maryland 21702-5012

10. SPONSOR/MONITOR'S ACRONYM(S)

11. SPONSOR/MONITOR'S REPORT NUMBER(S)

12. DISTRIBUTION / AVAILABILITY STATEMENT
Approved for Public Release; Distribution Unlimited

13. SUPPLEMENTARY NOTES

14. ABSTRACT

We examined if BRCA1 is involved in MEC differentiation and how its dysfunction pertains to breast tumor pathogenesis. We demonstrated that BRCA1 mediates acinar differentiation of MEC using 3-D culture. Reduction of BRCA1 by RNAi impairs acinus formation but enhances proliferation. Such aberrations can be rescued by expression of wild-type BRCA1 as well as a mutant in the central domain but not in the C-terminal BRCT domain, suggesting that the BRCT domain has a critical role in this process. Consistently, depletion of BRCA1 up-regulates the gene expression for proliferation but down-regulates that for differentiation. Moreover, application of the medium conditioned by differentiating normal MEC can reverse the phenotype of differentiation-defective breast cancer cells bearing reduced BRCA1 functions. This result implies BRCA1 is involved in secretion of certain paracrine/autocrine factors that induce MEC differentiation in response to extracellular matrix signals.

15. SUBJECT TERMS
breast tumor, mammary epithelial cells, BRCA1, differentiation, angioigenesis

16. SECURITY CLASSIFICATION OF:			**17. LIMITATION OF ABSTRACT**	**18. NUMBER OF PAGES**	**19a. NAME OF RESPONSIBLE PERSON**
					USAMRMC
a. REPORT	**b. ABSTRACT**	**c. THIS PAGE**			**19b. TELEPHONE NUMBER** *(include area code)*
U	U	U	UU	67	

Standard Form 298 (Rev. 8-98)
Prescribed by ANSI Std. Z39.18

Table of Contents

INTRODUCTION

BRCA1 participates in DNA damage repair, cell-cycle checkpoint control and transcriptional regulation, serving as a tumor suppressor to maintain genomic stability. BRCA1 is also involved in developmental processes[2-4] and exhibits a temporal and spatial expression pattern. In mammary tissue, BRCA1 is upregulated in rapidly dividing, differentiating cells but downregulated in regressing cells[5]. Mouse mammary tissue with a conditional *Brca1* knockout displays abnormal ductal morphogenesis and breast tumor[6], providing circumstantial evidence for BRCA1 participating in mammary epithelial cell (MEC) differentiation.

In the past year, we examined if BRCA1 is involved in MEC differentiation and how its dysfunction pertains to breast tumor pathogenesis. The published research article[1] is attached as an appendix. We demonstrated that BRCA1 mediates acinar differentiation of MEC using 3-D culture. Reduction of BRCA1 by RNAi impairs acinus formation but enhances proliferation. Such aberrations can be rescued by expression of wild-type BRCA1 as well as a mutant in the central domain but not in the C-terminal BRCT domain, suggesting that the BRCT domain has a critical role in this process. Consistently, depletion of BRCA1 up-regulates the gene expression for proliferation but down-regulates that for differentiation. Moreover, application of the medium conditioned by differentiating normal MEC can reverse the phenotypes of differentiation-defective breast cancer cells bearing reduced BRCA1 functions. This result implies BRCA1 is involved in secretion of certain paracrine/autocrine factors that induce MEC differentiation in response to extracellular matrix signals. This study summarizes the data associated with tasks outlined in **Aim1** and partly in **Aims 2** and **3**.

BODY

RESEARCH DESIGN, METHODS AND DATA

1. Determine the requirement of BRCA for MEC differentiation. We adopted 3-D culture system using Matrigel to observe acinar morphogenesis of MEC. BRCA1-depleted MCF10A cells were established by expressing adenoviral BRCA1-RNAi and subjected to a 3-D morphogenesis assays, in comparison with luciferase-RNAi-treated cells as a control. We determined the region of BRCA1 protein involved in MEC differentiation.

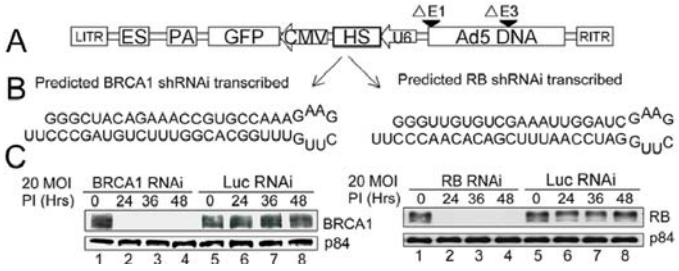

Fig.1. Construction of adenovirus-based shRNAi vector. *(A)* Diagram of the recombinant adenovirus construct expressing BRCA1- or RB-RNAi. Transcriptional units including U6 promoter–RNAi cassette (0.4 kb) and CMV-GFP (1.6 kb) as a marker were arranged as diagramed. PA: poly A signal, HS: targeted sequence of RNAi, LITR: left inverted terminal repeat, RITR: right inverted terminal repeat of adenovirus. (middle) *(B)* The predicted structure of a short hairpin RNA for BRCA1 (left) or RB (right). *(C)* Diminished expressions of BRCA1 (left) and RB (right) in HeLa cells after infected with the corresponding adenovirus-based RNAi. By western analyses, the BRCA1 (left) or RB (right) level was determined with an anti-RB antibody 0, 24, 36, or 48h post-infection at 20 MOI. The p84 protein serves as an internal loading control[1].

1a. Establish MCF10A human MEC transiently or stably expressing the BRCA siRNA to knockdown the cognate gene.

Generation of Adenovirus Expressing the BRCA1- or RB-RNAi. We generated an adenoviral RNAi vector that expressed a short-hairpin RNA (shRNA) against BRCA1 (Fig.1B, left) or RB (Fig.1B, right) for comparison under a U6 promoter. This adenoviral vector co-expressed green fluorescence protein (GFP) as a reporter for the infection efficiency (Fig.1A). The knockdown potency of the RNAi vector was confirmed by western analysis on BRCA1 (Fig.1C, left) or RB (Fig.1C, right).

1b. Perform the 3-D morphogenesis assays on MEC with the knockdowned BRCA expression.

BRCA1-depleted MEC Failed to Form Acinus Structure. Mammary acinus is a polarized spherical structure of a single epithelial cell layer surrounding the lumen[7,8]. Morphogenesis of luciferase

(control)-, BRCA1- or RB-depleted cells was monitored in 3-D culture with Matrigel serving as a basement membrane matrix for mammary acinus formation. After 15h, control (Fig.2A.a1) and RB-depleted (Fig.2A.c1) cells exhibited active migratory behaviors, as characterized by outward projections from individual cells, possibly for cell-to-cell communication. In contrast, BRCA1-depleted cells appeared immotile, retaining the original spherical shape of single cells (Fig.2A.b1). After 4 days, control (Fig.2A.a2) and RB-depleted (Fig.2A.c2) cells had started to form localized, primordial acinus structures, whereas BRCA1-depleted cells (Fig.2A.b2) had started to exhibit horizontal spreading on the surface of Matrigel. After 7 days, control (Fig.2A.a3) and RB-depleted (Fig.2A.c3) cells had formed almost complete acini with the appearance of the central hollow lumens, as confirmed by confocal sectioning. On the other hand, BRCA1-depleted cells (Fig.2A.b3) had formed irregular shaped aggregates embedded in a lawn of cells. In 20 days, control (Fig.2B.a) and RB-depleted (data not shown) cells formed the organized acinus structure of a single luminal layer surrounding a hollow lumen. Conversely, the BRCA1-depleted cells formed large irregular-shaped multilobular structures with the completely filled lumen (Fig.2B.b), similar to that was observed by the activation of an oncogene ErbB2[7,9].

1c. Test if the normal phenotype of the mammary acinar structure is restored by the ectopically expressed wild-type or point mutant forms of the siRNA-resistant BRCA.

The Normal MEC Acinus Formation is Rescued by RNAi-resistant Wild-type BRCA1. To validate that the ablated acinus formation was solely due to the absence of the functional BRCA1, it was tested if reintroduction of wild-type BRCA1, by means of a plasmid expressing the RNAi-resistant wild-type BRCA1, could rescue the normal phenotype. In this vector, silent mutations were generated within the RNAi target sequence to confer the resistance (Fig 3A.a,b). The efficiency of the RNAi resistance was confirmed by western analysis, showing the expression of wild-type BRCA1 was maintained in HeLa cells transfected with the RNAi-resistant BRCA1 vector prior to the RNAi treatment (Fig.3A.c). The 3-D morphogenesis assay was conducted on MCF10A cells pretreated with the RNAi-resistant wild-type BRCA1 vector then infected with either control luciferase- or BRCA1-RNAi adenovirus (Fig.3B.a,b). The presence of the RNAi-resistant BRCA1 rescued the normal acinus formation, as the phenotypes of those treated with the control- (Fig.3B.a) and BRCA-RNAi (Fig.3B.b) were almost indistinguishable at all the time points monitored. The central hollow lumens became evident in a week, as confirmed by confocal sectioning. Overall, these results provided evidence that BRCA1 is essential for the normal acinar morphogenesis of MEC.

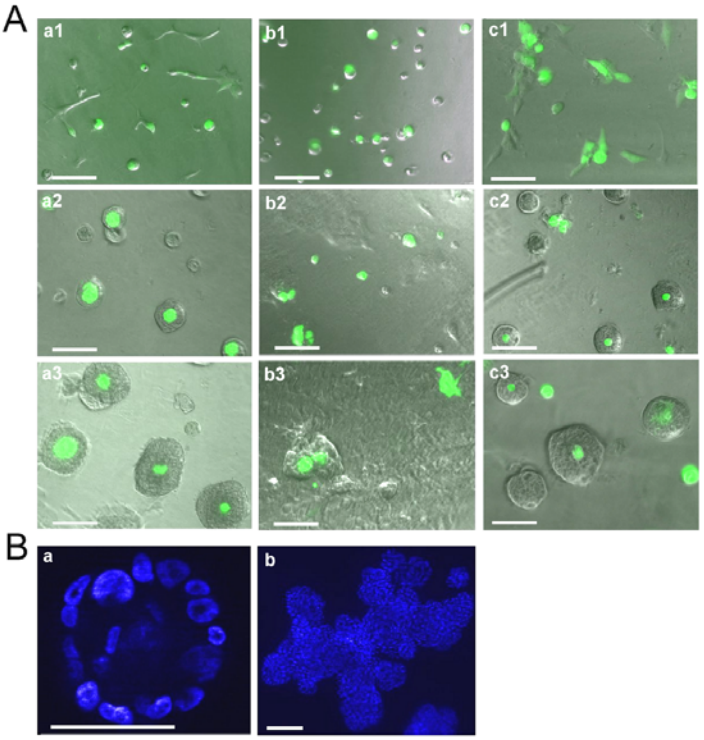

Fig.2. Abnormal acinar morphogenesis of MCF10A cells depleted of BRCA1 expression. *(A)* MCF10A cells were infected with 20 MOI of adenovirus expressing control luciferase- (a), BRCA1- (b), or RB-RNAi (c) and acinar morphogenesis was captured by GFP/phase signal at different time points [(1) 15h, (2) 4 days, (3) and 7 days] of growth in 3-D culture. *(B)* DAPI stained control (a) and BRCA1-deficient cells (b) after 20 days in 3-D culture. The bottom bar equals 50 μm[1].

RNAi-resistant M1775R Mutant BRCA1 Failed to Rescue the Acinus Formation. To further test the wild type BRCA1 is essential for acinus formation, we introduced two naturally occurring point mutations into the RNAi-resistant BRCA1 construct, Q356R in the RAD50/ZBRK1 binding region and

M1775R in BRCT domain. The 3-D morphogenesis assay was conducted on MCF10A cells pretreated with the RNAi-resistant point-mutant BRCA1 vector then infected with BRCA1-RNAi adenovirus (Fig.3B.c,d). The RNAi-resistant BRCA1 carrying Q356R (Fig.3B.c) mutation rescued the normal acinus formation with the appearance of the central hollow lumen in a week of growth. On the other hand, the RNAi-resistant BRCA1 carrying M1775R mutation (Fig.3B.d) failed to rescue, suggesting that BRCT domain of BRCA1 is important for mediating the acinus formation.

MEC proliferates in the Absence of Functional BRCA1. Next, to verify if the loss of the functional BRCA1 leads to the cellular proliferation, cells were recovered from the Matrigel after one week of growth and the number of viable cells was counted (Fig.3C). The populations of cells which formed the normal acinus structures had the cell numbers 2~3 times that originally seeded, suggesting that cells had divided at least once before committing themselves to differentiate, in a manner comparable to adipocyte differentiation mediated by RB[10]. On the other hand, the populations which failed to form the acinus structures had the cell numbers 6~8 times the original, suggesting that these cells continued dividing during the course of the experiment. This result reflects the fact that cellular differentiation and proliferation are opposing signaling events[8], and the presence of the functional BRCA1 seems essential for driving cells into the differentiation pathway.

2. Identify the downstream effectors regulated by BRCA during the differentiation of MEC. BRCA-depleted MCF10A cells were grown in the 3-D cultures, and the gene expression profiles were compared to that of control (luciferase-RNAi-treated) cells using microarray.

2a. Collect the gene transcripts/cell lysates from the MEC grown in the 3-D cultures and compare the gene/protein expression profiles between the cells in the presence and in the absence of BRCA using microarrays/2-D PAGE.

2b. Identify the genes/proteins with significantly altered expression levels in the absence of BRCA and prepare their antibodies.

Loss of BRCA1 at the initial stage of acinar morphogenesis up-regulates the expression of proliferation but down-regulates differentiation genes. To assess the differential gene expression pattern caused by the loss of BRCA1 at the initial stage of acinar morphogenesis, we performed pair-wise microarray analyses on MCF10A cells infected with the control luciferase- or BRCA1-RNAi adenovirus and grown in 3-D cultures for 15h (Table 1). The result confirmed that BRCA1-RNAi largely decreased the BRCA1 level (-7.9 folds). In BRCA1-depleted cells, a mammary differentiation factor STAT5B[11] and a

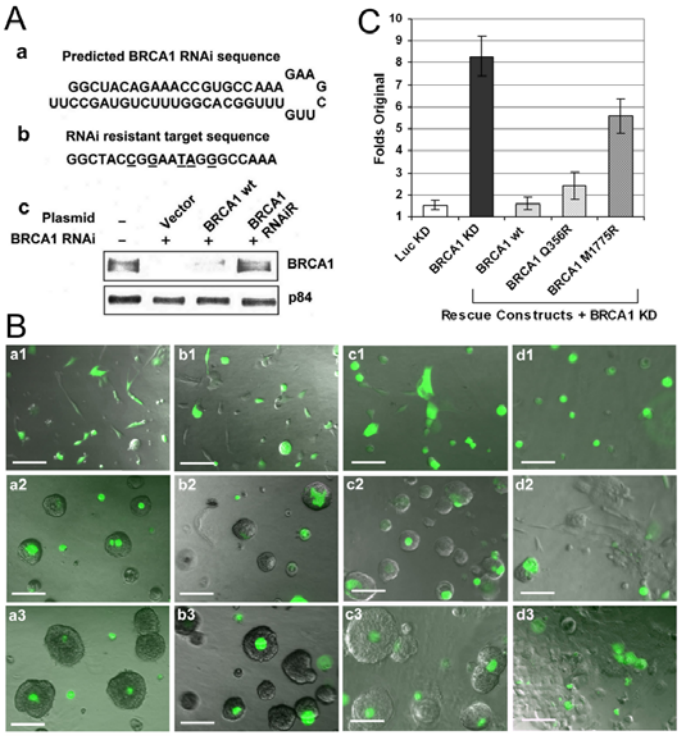

Fig.3. Restoration of the normal acinar morphogenesis by introducing the RNAi-resistant BRCA1. *(A)* Construction of RNAi-resistant BRCA1. a. The predicted structure of a short hairpin RNA for BRCA1. b. Nucleotides substituted in the vector expressing the RNAi-resistant BRCA1. c. Pretreatment with the RNAi-resistant BRCA1 rescued the BRCA1 expression in HeLa cells after infected with the adenovirus-based BRCA1 RNAi. The p84 protein serves as an internal loading control. *(B)* MCF10A cells were transfected with a vector expressing the RNAi resistant wild-type (a,b), Q356R (c), or M1775R (d) point mutant of BRCA1 and infected with 20 MOI of adenovirus expressing control luciferase- (a) or BRCA1-RNAi (b-e). The acinar morphogenesis was detected by GFP/phase signal at different time points [(1) 15h, (2) 4 days, and (3) 7 days] in 3-D culture. The bottom bar equals 50 μm. *(C)* MCF10A cells recovered from 3-D culture after one week and the percentage viable cell numbers with respect to that originally plated were calculated. Luc KD: cells infected with control luciferase-RNAi. BRCA1-KD: cells infected with BRCA1-RNAi. BRCA1-wt: cells pretreated with RNAi-resistant wild-type BRCA1 prior to infection with BRCA1-RNAi. BRCA1-Q356R: cells pretreated with RNAi-resistant Q356R point mutant BRCA1 prior to infection with BRCA1-RNAi. BRCA1-M1775R: cells pretreated with RNAi-resistant M1775R point mutant BRCA1 prior to infection with BRCA1-RNAi[1].

caretaker/cancer susceptibility gene FANCA[12], as well several interferon- or caspase-associated proteins, were down-regulated. Concomitantly, in these cells, certain proliferation markers, including HMGA2[13], angiopoietin-1[14] and CaM kinase II β[15], were up-regulated. The data suggests that the gene expression pattern of BRCA1-depleted cells at the initial stage of acinar morphogenesis is overall directed toward proliferation rather than differentiation, supporting our phenotypic observation that the BRCA1-depleted MEC failed to enter the acinus forming pathway but instead proceeded to proliferate.

Category	Gene Symbol	Gene ID	Name	Folds
Membrane Associated Protein	CLCN4	W26966	chloride channel 4	+ 4.8
	CLECSF12	AF400600	C-type (calcium dependent, carbohydrate-recognition domain) lectin,	+ 3.6
	CT120	NM_024792	membrane protein expressed in epithelial-like lung adenocarcinoma	- 3.0
	TTYH3	AI934753	tweety homolog 3 (Drosophila), maxi-Cl – channel	- 4.2
	VAMP3	NM_004781	vesicle-associated membrane protein 3 (cellubrevin)	- 9.3
Transcriptional Regulation	HMGA2	NM_003483	high mobility group AT-hook 2 /// high mobility group AT-hook 2	+ 4.6
	HRMT1L1	AI928367	HMT1 hnRNP methyltransferase-like 1 (S. cerevisiae)	- 3.0
	STAT5B	BE645861	signal transducer and activator of transcription 5B	- 2.4
	TFDP1	AW007021	transcription factor Dp-1	- 3.2
	BRCA1	NM_007295	breast cancer 1, early onset	- 7.9
Signaling	ANGPT1	NM_001146	angiopoietin 1	+ 2.7
	CAMK2B	U23460	calcium/calmodulin-dependent protein kinase (CaM kinase) II beta	+ 2.5
	TRAF3	AI721219	TNF receptor-associated factor 3	- 3.0
	IFNAR1	AA133989	interferon (alpha, beta and omega) receptor 1	-3.1
	PDXK	AW449022	pyridoxal (pyridoxine, vitamin B6) kinase	- 4.0
	HTATIP2	BC002439	HIV-1 Tat interactive protein 2, 30kDa	- 4.1
	CARD10	AY028896	caspase recruitment domain family, member 10	- 4.2
	RAB34	AF322067	RAB34, member RAS oncogene family	- 4.7
	GM2A	AL513583	GM2 ganglioside activator protein	- 14.6
Cytoskeleton	TPX2	AF098158	TPX2, microtubule-associated protein homolog (Xenopus laevis)	-3.8
Enzyme	IDS	BF346014	iduronate 2-sulfatase (Hunter syndrome)	+3.6
	USP49	NM_004275	ubiquitin specific protease 49	-3.9
	ICMT	AL578502	isoprenylcysteine carboxyl methyltransferase	-4.1

Table 1. Genes up- or down-regulated in BRCA1-depleted MCF10A cells ($p < 0.05$)[1].

3. Investigate how BRCA regulates the expression of the effectors during MEC differentiation. Our microarray result showed that depletion of BRCA1 in MEC during 15 h of growth in 3-D matrix altered the expression profiles of various genes. Then, we hypothesized that BRCA1 is involved in transcriptional regulation of certain genes essential for MEC differentiation. Fortuitously, we found that application of medium conditioned by wild-type MEC was able to revert the phenotype of BRCA1-depleted MEC into that normally differentiated in 3-D matrix. This observation suggests that specific factors are secreted by differentiating MEC which function in a paracrine/autocrine fashion.

Conditioned Medium from Differentiating MEC Rescue the Acinus-forming Phenotype of Differentiation-defective MEC. Because the transfection efficiency in MCF10A cells usually reach around 30-50%, it was surprising to observe that the cells transfected with wild-type, as well as Q356R point mutant, BRCA1 rescued the acinus formation phenotype (Fig.3). Then, we speculated that certain factor(s) released from BRCA1 positive cells might have influenced the morphogenesis of the neighboring BRCA1-negative cells. To test this possibility, the conditioned medium collected from MCF10A cells, which has been infected with luciferase-RNAi/GFP adenovirus, was used to plate and continually (every 15h) feed BRCA1-RNAi/GFP adenovirus-infected MCF10A cells in 3-D culture. In contrast to BRCA1-depleted cells with the fresh growth medium (Fig.4A.a), about ~20% of BRCA1-depleted cells fed with the conditioned medium was able to resume the acinus forming phenotype (Fig.4A.b). This observation suggests that MCF10A cells secrete certain paracrine/autocrine factor(s) in response to ECM signals whereas cells depleted of BRCA1 lack such the activity. Next, we tested if the administration of the condition medium from the differentiating MCF10A cells can alter the growth and morphology of breast cancer cells lain in 3-D cultures (Fig.4B). Two different breast carcinoma cell lines were tested: HCC1937 (Fig.4B.a,b), which expresses a truncated form of BRCA1 at one of the C-

terminal BRCT domain[16] and SKBR3 (Fig.4B.c,d), which expresses a low basal level of BRCA1[17]. Both cancer cells lain in 3-D culture with the fresh growth medium, formed irregular shaped large aggregates (Fig.4B.a,c). Conversely, when these cancer cells were continually (every 12h) fed with the conditioned growth medium from differentiating MCF10A cells, a large fraction of the cell population (>40%) formed acinus-like spherical structures (Fig.4B.b,d) with the appearance of the central hollow lumen in a week. In addition, a significant number of dead cells were observed among those incapable of forming acinus-like structure (~60%). After a week of growth, the number of viable cells was counted (Fig.4C). BRCA1-depleted MCF10A cells was ~40% lower in those treated with the conditioned medium than the untreated. Also, the two cancer cell lines tested were at least 60% lower in those treated with the conditioned medium than the untreated. These observations suggest that the differentiating MCF10A cells, in response to ECM signals, secrete certain paracrine/autocrine factors, which promote differentiation for the non-malignant/malignant MEC that have reduced BRCA1 functions.

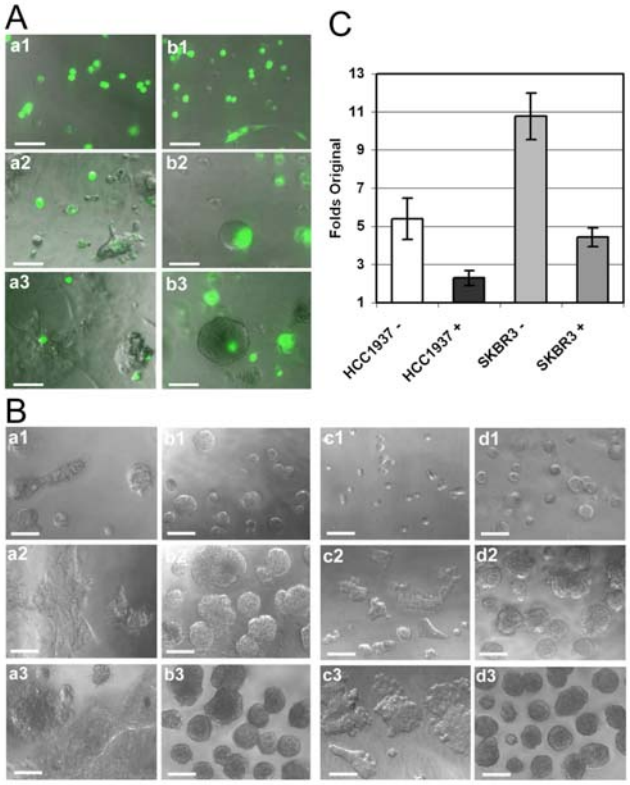

Fig.4. Conditioned medium from differentiating MEC revert the phenotypes of acinus formation-defective MEC. *(A)* MCF10A cells were infected with 20 MOI of adenovirus expressing the control luciferase RNAi or BRCA1 RNAi (a,b). Cells were fed every 15h with the fresh medium (a) or conditioned medium from the control cells (b). The acinar morphogenesis was monitored at different time points [(1) 15h, (2) 4 days, (3) and 7 days] of growth in 3-D culture. The bottom bar equals 50 μm. *(B)* Breast cancer cells (a.b: HCC1937 and c,d: SKBR3) were fed every 12h with the fresh growth medium (a,c) or conditioned medium from differentiating MCF10A cells (b,d). The acinar morphogenesis was monitored at different time points [(1) 15h, (2) 4 days, (3) and 7 days] of growth in 3-D culture. The bottom bar equals 50 μm. *(C)* MEC with different manipulations were recovered from 3-D culture after one week of growth in the absence (-) or presence (+) of conditioned medium, and the percentage viable cell numbers with respect to that originally plated were calculated[1].

Tasks in Progress:

Aim2c. ***Monitor the expression patterns of the effectors during MEC differentiation.*** We will focus on secreted factors with expression patterns altered between the normally differentiating wild-type MEC and those depleted of BRCA1. We will perform mass spectrometry to analyze the expression patterns of proteins in the conditioned media and evaluate if they are essential for MEC differentiation by immunodepletion.

Aim3. Investigate how BRCA regulates the expression of the effectors during MEC differentiation.

3a. Test the involvement of the effector genes in MEC differentiation by gene KD or overexpression.
3b. Perform reporter assays to test the transcriptional regulations of the effector genes by ectopically expressed BRCA1.
3c. Determine the region of BRCA responsible for the transcriptional regulation of the effector genes by reporter assays using different BRCA point mutants.

Among the genes with altered expression profiles upon depletion of BRCA1 in MEC (Table 1), we focused on angiopoietin-1 (ANG1), a secreted angiogenic factor, as an extension of tasks proposed. Although it is so far unknown if ANG1 directly influences MEC differentiation, ANG1 contributes to tumor progression by modulating the tumor microenvironment by angiogenesis. ANG1 expression increased as BRCA1 level decreased in MEC, suggesting its potential repression by BRCA1. Our result showed that ANG1 transcription is directly repressed by BRCA1, which forms a repressor complex with ZBRK1 and CtIP transcriptional repressors on *ANG1* promoter, delineating a significance of

transcriptional regulation by BRCA1 for tumor suppression function. Our data also demonstrated that ANG1 upregulation promotes vascular maturation and exacerbates the malignancy of Brca1-associated mouse breast tumors. These data have been compiled into a research article[18], which is attached as an appendix.

To complete the tasks outlined in **Aim3a-c**, we will test if factors, secreted by differentiating MEC and essential for paracrine/autocrine induction of differentiation (**Aim2c**), are transcriptionally regulated by BRCA1 by using approaches similar to those adopted for studying ANG1 regulation[18].

KEY RESEARCH ACCOMPLISHMENTS

- We have demonstrated that BRCA1 is involved in MEC differentiation and its impairment leads to proliferation. Such aberrations may serve as a pathogenic basis for BRCA1-associated breast tumors.
- We have shown that a differentiation-defective, malignant phenotype of BRCA1-associated breast cancer cells can be reverted by application of the conditioned medium from normally differentiating MEC. This finding suggests a role for BRCA1 in secretion of factors that promote differentiation in a paracrine/autocrine fashion and their potential therapeutic application to breast cancer.
- We also have demonstrated that an impaired transcriptional regulatory activity of BRCA1 plays a major role in tumor progression contributed by enhanced angiogenesis.

REPORTABLE OUTCOMES

- Publications:
    - Furuta, S., Jiang, X., Gu, B., Cheng, E., Chen, P. L., and Lee, W. H. (2005). Depletion of BRCA1 impairs differentiation but enhances proliferation of mammary epithelial cells. Proc Natl Acad Sci USA *102*, 9176-9181.
    - Furuta, S., Wang, J. M., Wei, S., Jeng, Y. M., Jiang, X., Gu, B., Chen, P. L., Lee, E. Y-H. P., Lee, W. H. (2006) Removal of BRCA1/CtIP/ZBRK1 repressor complex on *ANG1* promoter leads to accelerated breast tumor growth contributed by prominent vasculature. [Submitted]

- Presentations:
    - UCI Biological Chemistry Departmental Annual Research Seminar: oral presentation 1st prize (June, 2005)
    - UCI Biological Chemistry Departmental Annual Retreat: oral presentation 2nd prize (Oct. 2005)

CONCLUSIONS

Our data demonstrated that reduction of BRCA1 by RNAi impairs acinus formation but enhances proliferation of MEC, and the C-terminal BRCT domain plays a critical role in this process. BRCA1 depletion up-regulates the gene expression for proliferation but down-regulates that for differentiation. Moreover, application of the medium conditioned by normally differentiating MEC can reverse the phenotype of differentiation-defective, BRCA1-deficient MEC, suggesting that BRCA1 is involved in secretion of certain paracrine/autocrine factors that induce MEC differentiation in 3-D matrix.

REFERENCES

1. Furuta, S. et al. Depletion of BRCA1 impairs differentiation but enhances proliferation of mammary epithelial cells. *Proc. Natl. Acad. Sci. USA* **102**, 9176-9181 (2005).

2. Hakem, R. et al. The tumor suppressor gene Brca1 is required for embryonic cellular proliferation in the mouse. *Cell* **85**, 1009-1023 (1996).

3. Liu, C.Y., Flesken-Nikitin, A., Li, S., Zeng, Y. & Lee, W.H. Inactivation of the mouse Brca1 gene leads to failure in the morphogenesis of the egg cylinder in early postimplantation development. *Genes Dev.* **10**, 1835-1843 (1996).

4. Lane, T.F. et al. Expression of Brca1 is associated with terminal differentiation of ectodermally and mesodermally derived tissues in mice. *Genes Dev.* **9**, 2712-2722 (1995).

5. Marquis, S.T. et al. The developmental pattern of Brca1 expression implies a role in differentiation of the breast and other tissues. *Nat. Genet.* **11**, 17-26 (1995).

6. Xu, X. et al. Conditional mutation of Brca1 in mammary epithelial cells results in blunted ductal morphogenesis and tumour formation. *Nat. Genet.* **22**, 37-43 (1999).

7. Debnath, J., Muthuswamy, S.K. & Brugge, J.S. Morphogenesis and oncogenesis of MCF-10A mammary epithelial acini grown in three-dimensional basement membrane cultures. *Methods* **30**, 256-268 (2003).

8. Weaver, V.M. & Bissell, M.J. Functional culture models to study mechanisms governing apoptosis in normal and malignant mammary epithelial cells. *J Mammary Gland Biol Neoplasia* **4**, 193-201 (1999).

9. Debnath, J. et al. The role of apoptosis in creating and maintaining luminal space within normal and oncogene-expressing mammary acini. *Cell* **111**, 29-40 (2002).

10. Chen, P.L., Riley, D.J., Chen, Y. & Lee, W.H. Retinoblastoma protein positively regulates terminal adipocyte differentiation through direct interaction with C/EBPs. *Genes Dev.* **10**, 2794-2804 (1996).

11. Liu, X., Robinson, G.W., Gouilleux, F., Groner, B. & Hennighausen, L. Cloning and expression of Stat5 and an additional homologue (Stat5b) involved in prolactin signal transduction in mouse mammary tissue. *Proc. Natl. Acad. Sci.* **92**, 8831-8835 (1995).

12. Folias, A. et al. BRCA1 interacts directly with the Fanconi anemia protein FANCA. *Hum. Mol. Genet.* **11**, 2591-2597 (2002).

13. Tessari, M.A. et al. Transcriptional activation of the cyclin A gene by the architectural transcription factor HMGA2. *Mol. Cell Biol.* **23**, 9104-9116 (2003).

14. Caine, G.J., Blann, A.D., Stonelake, P.S., Ryan, P. & Lip, G.Y.H. Plasma angiopoietin-1, angiopoietin-2 and Tie-2 in breast and prostate cancer: a comparison with VEGF and Flt-1. *Eur. J. Clin. Invest.* **33**, 883-890 (2003).

15. Kahl, C.R. & Means, A.R. Regulation of Cell Cycle Progression by Calcium/Calmodulin-Dependent Pathways. *Endocr. Rev.* **24**, 719-736 (2003).

16. Yu, X., Chini, C.C.S., He, M., Mer, G., Chen, J. The BRCT domain is a phospho-protein binding domain. *Science* **302**, 639-42 (2003).

17. Blagosklonny, M.V., An, W.G., Melillo, G.M., Nguyen, P., Trepel, J.B., Meckers, L.M. Regulation of BRCA1 by protein degradation. *Oncogene* **18**, 6460-8 (1999).

18. Furuta, S. et al. Removal of BRCA1/CtIP/ZBRK1 repressor complex on ANG1 promoter leads to accelerated breast tumor growth contributed by prominent vasculature. *[Submitted]* (2006).

APPENDICES

1. Furuta, S., Jiang, X., Gu, B., Cheng, E., Chen, P. L., and Lee, W. H. (2005). Depletion of BRCA1 impairs differentiation but enhances proliferation of mammary epithelial cells. Proc Natl Acad Sci USA *102*, 9176-9181.

2. Furuta, S., Wang, J. M., Wei, S., Jeng, Y. M., Jiang, X., Gu, B., Chen, P. L., Lee, E. Y-H. P., Lee, W. H. (2006) Removal of BRCA1/CtIP/ZBRK1 repressor complex on *ANG1* promoter leads to accelerated breast tumor growth contributed by prominent vasculature. [Submitted]

Depletion of BRCA1 impairs differentiation but enhances proliferation of mammary epithelial cells

Saori Furuta, Xianzhi Jiang, Bingnan Gu, Eric Cheng, Phang-Lang Chen, and Wen-Hwa Lee*

Department of Biological Chemistry, College of Medicine, University of California, Irvine, CA 92697

Communicated by Douglas C. Wallace, University of California, Irvine, CA, May 19, 2005 (received for review March 1, 2005)

Cumulative evidence indicates that breast cancer-associated gene 1 (*BRCA1*) participates in DNA damage repair and cell-cycle checkpoint control, serving as a tumor susceptibility gene to maintain the global genomic stability. However, whether BRCA1 has a direct role in cell proliferation and differentiation, two key biological functions in tumorigenesis, remains unclear. Here we demonstrate BRCA1 mediates differentiation of mammary epithelial cell (MEC) for acinus formation by using the *in vitro* 3D culture system. Reduction of *BRCA1* in MEC by RNA interference impairs the acinus formation but enhances proliferation. Such aberrations can be rescued by expression of wild-type BRCA1 as well as a mutant at the RAD50-binding domain but not at the C-terminal BRCT domain, suggesting that the C-terminal BRCT domain has a critical role in these processes. Consistently, depletion of BRCA1 up-regulates the gene expression for proliferation but down-regulates that for differentiation. Moreover, application of the medium conditioned by differentiating normal MEC can reverse the phenotypes of differentiation-defective breast cancer cells bearing reduced BRCA1 functions. Our observation implies BRCA1 is involved in secretion of certain paracrine/autocrine factors that induce MEC differentiation in response to extracellular matrix signals, providing, in part, an explanation for the etiological basis of either sporadic or familial breast cancer due to the loss or reduction of BRCA1.

breast cancer | tumor suppressor | 3D culture | matrix gel

Mutations in the breast cancer susceptibility gene *breast cancer-associated gene 1* (*BRCA1*) account for up to half of hereditary breast cancer cases (1, 2) and almost all hereditary breast and ovarian cancer cases (3). Also, decreased *BRCA1* expression is often found during sporadic breast cancer progression (4). Despite that a tissue-specific role of BRCA1 in breast and ovary is speculated (3), the cumulated evidence primarily converges on its universal functions, DNA damage repair, cell-cycle checkpoint control, and transcriptional regulation, to maintain genomic stability (3).

The BRCA1 protein encompasses distinctive modules to interact with various proteins of diverse functions (5, 6). The N terminus possesses a RING finger domain, which dimerizes with BARD1 to exhibit ubiquitin ligase activity (5). The central region possesses two nuclear localization signals (5) and interacts with the DNA damage repair complex RAD50/MRE11/NBS1, transcription repressor ZBRK1, and BRCA2 (3, 6, 7). The C terminus possesses two tandem repeats of the BRCT motif, which is commonly found in DNA repair proteins (5) and interacts with CtIP, HDAC, and BACH1 (6, 8, 9). Loss of BRCA1 function leads to genomic instability, which diverges into two consequences (10). One is to trigger cell cycle arrest and apoptosis through activation of p53 (10). Alternatively, *BRCA1* deficiency perturbs the chromosomal integrity (11) and increases the mutation rate of other genes (10). Breast tumors from the *BRCA1* germ-line mutation carriers often display the allelic loss of tumor suppressors *p53* and *PTEN* (12), as well as the overexpression of oncogenes *ErbB2* and *c-Myc* (13). These findings endorse the role of BRCA1 in the maintenance of genomic integrity and the relevance of its loss to proliferation and tumorigenicity.

Nevertheless, it remains unresolved why *BRCA1* germ-line mutations exert malignancy mainly in breast and ovary. It was reported that BRCA1 expression is spatially and temporally regulated at the distinct stages of mammary gland development (14). Furthermore, conditional *Brca1* knockout mice display incomplete and abnormal ductal morphogenesis and, after latency, mammary tumor (15), providing circumstantial evidence for BRCA1 participating in MEC differentiation.

In this communication, we show that the reduction of BRCA1 expression by RNA interference (RNAi) causes a failure of mammary acinus formation but enhances the proliferation of mammary epithelial cell (MEC) using an *in vitro* 3D culture system, a close resemblance to *in vivo* environment allowing different cell types to colocalize and coordinate in the extracellular matrix (ECM) (16–18). This observation, at least in part, delineates the tumor suppressor function of BRCA1 in mediating MEC differentiation and the etiological relevance of the defect.

Materials and Methods

Adenovirus-Based RNAi Vector Construction. The adenovirus-based RNAi vector was generated by subcloning the transcriptional unit of U6 promoter-BRCA1 or -retinoblastoma (RB) short-hairpin RNAi (shRNAi) (0.4 kb) into pAdTrack plasmid upstream of the CMV-GFP cassette (1.6 kb) (19, 20). 293T cells were transfected with the recombinant adenoviral plasmid using lipofectin (Invitrogen), and adenovirus with the titer of 10^{10}-10^{12}/ml was collected.

Cell Cultures. Human normal MEC MCF10A was cultured in DMEM/F12 medium (Invitrogen), as described (16), whereas breast cancer cell lines HCC1937 and SKBR3 were cultured in high-glucose DMEM (Invitrogen), as described (16).

3D Morphogenesis Assay. MCF10A cells were infected with adenovirus-RNAi at 20 multiplicities of infection (moi) for 24 h. Approximately 3,500 infected cells per well were seeded in eight-well chamber slides coated with Growth Factor Reduced Matrigel (BD Biosciences) and covered with growth medium supplemented with 2% Matrigel as described (16). The 3D morphogenesis was monitored by fluorescence microscopy/confocal sectioning at 15-h intervals for 2–3 weeks. For experiments using the conditioned medium, medium collected from MCF10A cells infected with luciferase-RNAi virus was used to feed MCF10A cells infected with BRCA1-RNAi or two carcinoma cell lines, HCC1937 and SKBR3. Collection/application of the conditioned medium was performed every 12–15 h for 2 weeks. For cell number counting, cells were recovered from Matrigel after 1 week by digestion with dispase (BD Bio-

Abbreviations: BRCA1, breast cancer-associated gene 1; MEC, mammary epithelial cell(s); ECM, extracellular matrix; RNAi, RNA interference; moi, multiplicity of infection; shRNA, short-hairpin RNA; RB, retinoblastoma.

*To whom correspondence should be addressed. E-mail: whlee@uci.edu.

www.pnas.org/cgi/doi/10.1073/pnas.0503793102

sciences), following the manufacturer's instructions. The number of viable cells was measured by using the trypan blue exclusion method.

Fluorescence Imaging. Fluorescence imaging was performed on a Zeiss Axiovert 200 M equipped with Hamamatsu Photonics (Hamamatsu City, Japan) K.K. Deep Cooled Digital Camera (model C4742–80-12AG) by using AXIOVISION 4.2 software (Zeiss). The images of the hollow acinus structures of live or fixed/DAPI-stained cells were captured by the Z-stacking function for serial confocal sectioning at 2-μm intervals.

RNAi-Resistant BRCA1 Plasmid Construction. Cancer-linked point mutations of BRCA1 (Q356R and M1775R) were introduced into the cDNA by using a QuickChange site-directed mutagenesis kit (Stratagene). Within the wild-type BRCA1, the expression of which was driven by a CMV promoter in the CHpL vector (8), the nucleotides targeted by RNAi (nucleotides 385–405, 5′-GGCTACAGAAACCGAGCCAAA-3′) were partially substituted without changing the amino acid sequence (nucleotides 385–405, 5′-GGCTACCGGAATAGGGCCAAA-3′) by site-directed mutagenesis. The RNAi-resistant region was excised at NotI-EcoR and subcloned into each point mutant construct to replace the original sequence.

Microarray. MCF10A cells were infected with luciferase- or BRCA1-RNAi adenoviruses in duplicate at 20 moi for 24 h and seeded at 0.5×10^6 cells in each 60-mm plate coated with Growth Factor Reduced Matrigel (BD Biosciences) and covered with the growth medium supplemented with 2% Matrigel. After 15 h, cells were harvested from Matrigel by digestion with dispase, and RNA was extracted with TRIzol reagent (Invitrogen). cDNA was synthesized and labeled with biotin from 10 μg of the collected RNA and hybridized onto Affymetrix array (54,676 genes), stained with streptavidin–phycoerythrin and analyzed by using GCOS 1.2 software (Affymetrix) for multiplex pair-wise comparison provided by the University of California, Irvine, microarray core service. The statistical significance for each gene was evaluated by ANOVA single-factor analysis by using Microsoft EXCEL 2000, and the fold difference >2.3, as well as P value <0.05, was considered significant.

Results

Generation of Adenovirus Expressing the BRCA1- or RB-RNAi. To test whether BRCA1 has a direct role in proliferation and differentiation of MEC, we generated an adenovirus-based vector that expressed shRNA to knockdown the expression of *BRCA1* (Fig. 1*B Left*) under the control of the U6 promoter. Because the *RB* gene has an essential role in muscle, adipose, and neuronal tissue differentiation (21), RB expression depleted by shRNA (Fig. 1*B Right*) was used as a comparison. These adenoviral vectors coexpressed GFP as a reporter for infection efficiency (Fig. 1*A*). The knockdown potencies of these RNAi vectors were confirmed by Western blot analyses on the target proteins by using HeLa cells. The protein levels of BRCA1 (Fig. 1*C Left*) and RB (Fig. 1*C Right*) became undetectable after 24 h of infection with the corresponding adenovirus-RNAi at 20 moi. These adenovirus-based RNAi were used to deplete the expressions of BRCA1 and RB in normal MCF10A cells.

BRCA1-Depleted MEC Failed to Form Acinus Structure. The *in vitro* acinus is the polarized spherical structure of a single epithelial cell layer surrounding the lumen (16, 17). To capture the events critical for the normal acinus formation, the control, BRCA1-, and RB-depleted cells were plated in the 3D cultures, and their growths were monitored (Fig. 2). After 15 h, control (Fig. 2*Aa1*) and RB-depleted (Fig. 2*Ac1*) cells exhibited active migratory behaviors, as characterized by outward projections from individual cells, possibly for cell-to-cell communication. In contrast, BRCA1-depleted cells appeared immotile, retaining the original spherical shape of single cells (Fig. 2*Ab1*). After 4 days, control (Fig. 2*Aa2*) and RB-depleted (Fig. 2*Ac2*) cells had started to form localized primordial acinus structures, whereas BRCA1-depleted cells (Fig. 2*Ab2*) had started to exhibit horizontal spreading on the surface of Matrigel. After 7 days, control (Fig. 2*Aa3*) and RB-depleted (Fig. 2*Ac3*) cells had formed almost complete acini with the appearance of the central hollow lumens, as confirmed by confocal sectioning. On the other hand,

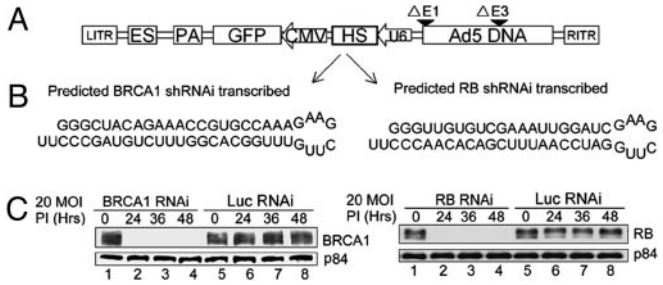

Fig. 1. Construction of the adenovirus-based shRNAi vector. (*A*) Diagram of the recombinant adenovirus construct expressing BRCA1- or RB-RNAi. Transcriptional units, including the U6 promoter-RNAi cassette (0.4 kb) and CMV-GFP (1.6 kb) as a marker, were arranged as diagrammed. PA, poly(A) signal; HS, targeted sequence of RNAi; LITR, left inverted terminal repeat; RITR, right inverted terminal repeat of adenovirus. (*B*) The predicted structure of a shRNA for BRCA1 (*Left*) or RB (*Right*). (*C*) Diminished expressions of BRCA1 (*Left*) and RB (*Right*) in HeLa cells after infection with the corresponding adenovirus-based RNAi. By Western analyses, the BRCA1 (*Left*) or RB (*Right*) level was determined with an anti-RB antibody 0, 24, 36, or 48 h postinfection at 20 moi. The p84 protein serves as an internal loading control.

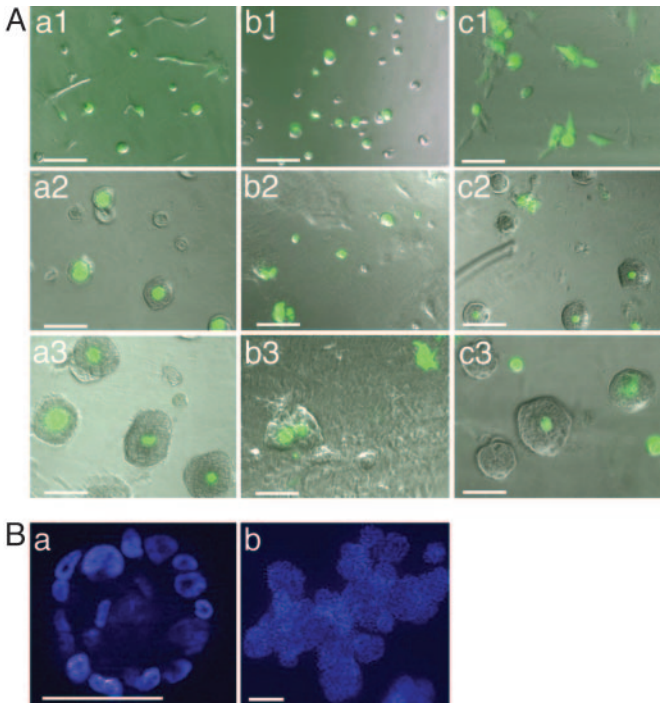

Fig. 2. Abnormal acinar morphogenesis of MCF10A cells depleted of BRCA1 expression. (*A*) MCF10A cells were infected with 20 moi of adenovirus-expressing control luciferase- (*a*), BRCA1- (*b*), or RB-RNAi (*c*), and acinar morphogenesis was captured by GFP/phase signal at different time points [(*1*) 15 h, (*2*) 4 days, and (*3*) 7 days] of growth in 3D culture. (*B*) DAPI-stained control (*a*) and BRCA1-deficient cells (*b*) after 20 days in 3D culture. (Bar, 50 μm.)

CELL BIOLOGY

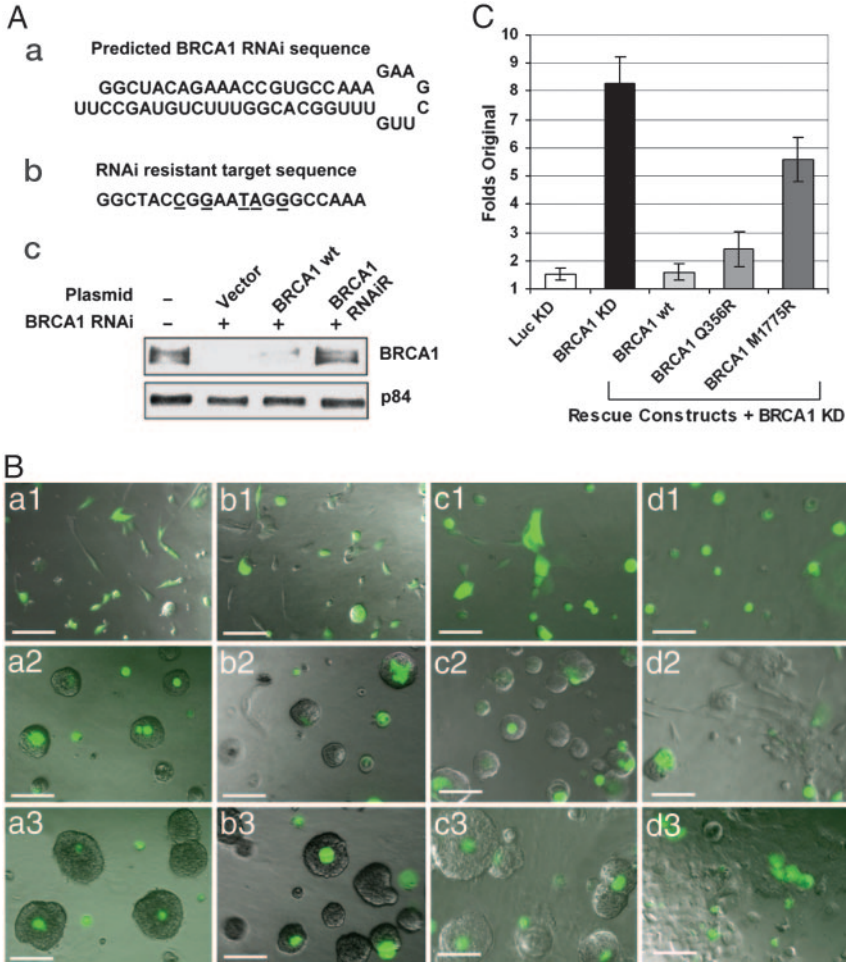

Fig. 3. Restoration of the normal acinar morphogenesis by introducing the RNAi-resistant BRCA1. (*A*) Construction of RNAi-resistant BRCA1. (*a*) The predicted structure of a shRNA for BRCA1. (*b*) Nucleotides substituted in the vector expressing the RNAi-resistant BRCA1. (*c*) Pretreatment with the RNAi-resistant BRCA1 rescued the BRCA1 expression in HeLa cells after infection with the adenovirus-based BRCA1 RNAi. The p84 protein serves as an internal loading control. (*B*) MCF10A cells were transfected with a vector expressing the RNAi-resistant wild-type (*a* and *b*), Q356R (*c*), or M1775R (*d*) point mutant of BRCA1 and infected with 20 moi of adenovirus expressing control luciferase- (*a*) or BRCA1-RNAi (*b–d*). The acinar morphogenesis was detected by GFP/phase signal at different time points [(*1*) 15 h, (*2*) 4 days, and (*3*) 7 days] in 3D culture. (Bar, 50 μm.) (*C*) MCF10A cells recovered from 3D culture after 1 week, and the percentage viable cell numbers with respect to that originally plated were calculated. Luc KD, cells infected with control luciferase-RNAi; BRCA1-KD, cells infected with BRCA1-RNAi; BRCA1-wt, cells pretreated with RNAi-resistant wild-type BRCA1 before infection with BRCA1-RNAi; BRCA1-Q356R, cells pretreated with RNAi-resistant Q356R point mutant BRCA1 before infection with BRCA1-RNAi; BRCA1-M1775R, cells pretreated with RNAi-resistant M1775R point mutant BRCA1 before infection with BRCA1-RNAi.

BRCA1-depleted cells (Fig. 2*Ab3*) had formed irregular-shaped aggregates embedded in a lawn of cells. In 20 days, control (Fig. 2*Ba*) and RB-depleted (data not shown) cells formed the organized acinus structure of a single luminal layer surrounding a hollow lumen. Conversely, the BRCA1-depleted cells formed large irregular-shaped multilobular structures with the completely filled lumen (Fig. 2*Bb*), similar to that observed by activation of an oncogene *ErbB2* (16, 18).

Normal MEC Acinus Formation Is Rescued by RNAi-Resistant Wild-Type BRCA1. To validate that the ablated acinus formation was solely due to the absence of the functional BRCA1, it was tested whether reintroduction of wild-type BRCA1, by means of a plasmid expressing the RNAi-resistant wild-type BRCA1, could rescue the normal phenotype. In this vector, silent mutations were generated within the RNAi target sequence to confer the resistance (Fig. 3 *Aa* and *Ab*). The efficiency of the RNAi resistance was confirmed by Western analysis, showing the expression of wild-type BRCA1 was maintained in HeLa cells transfected with the RNAi-resistant BRCA1 vector before the RNAi treatment (Fig. 3*Ac*). The 3D morphogenesis assay was conducted on MCF10A cells pretreated with the RNAi-resistant wild-type BRCA1 vector then infected with either control luciferase- or BRCA1-RNAi adenovirus (Fig. 3 *Ba* and *Bb*). The presence of the RNAi-resistant BRCA1 rescued the normal acinus formation, because the phenotypes of those treated with the control- (Fig. 3*Ba1–3*) and BRCA-RNAi (Fig. 3*Bb1–3*) were almost indistinguishable at all time points monitored. The central hollow lumens became evident in 1 week, as confirmed by confocal sectioning. Overall, these results provided evidence that BRCA1 is essential for the normal acinar morphogenesis of MEC.

RNAi-Resistant M1775R Mutant BRCA1 Failed to Rescue the Acinus Formation. To further test that wild-type BRCA1 is essential for acinus formation, we introduced two naturally occurring point mutations into the RNAi-resistant BRCA1 construct, Q356R in the RAD50/ZBRK1-binding region and M1775R in BRCT domain. The 3D morphogenesis assay was conducted on MCF10A cells pretreated with the RNAi-resistant point-mutant

Table 1. Genes up- or down-regulated in BRCA1-depleted MCF10A cells ($P < 0.05$)

Category	Gene symbol	Gene ID	Name	Folds changed
Membrane-associated protein	CLCN4	W26966	Chloride channel 4	+4.8
	CLECSF12	AF400600	C-type (calcium-dependent, carbohydrate-recognition domain) lectin, superfamily member 12, β-glucan receptor (BGR) 7	+3.6
	CT120	NM_024792	Membrane protein expressed in epithelial-like lung adenocarcinoma	−3.0
	TTYH3	AI934753	Tweety homolog 3 (*Drosophila*), maxi-Cl-channel	−4.2
	VAMP3	NM_004781	Vesicle-associated membrane protein 3 (cellubrevin)	−9.3
Transcriptional regulation	HMGA2	NM_003483	High-mobility group AT-hook 2///high-mobility group AT-hook 2	+4.6
	HRMT1L1	AI928367	HMT1 hnRNP methyltransferase-like 1 (*Saccharomyces cerevisiae*)	−3.0
	STAT5B	BE645861	Signal transducer and activator of transcription 5B	−2.4
	TFDP1	AW007021	Transcription factor Dp-1	−3.2
	BRCA1	NM_007295	Breast cancer 1, early onset	−7.9
Signaling	ANGPT1	NM_001146	Angiopoietin 1	+2.7
	CAMK2B	U23460	Calcium/calmodulin-dependent protein kinase (CaM kinase) II β	+2.5
	TRAF3	AI721219	TNF receptor-associated factor 3	−3.0
	IFNAR1	AA133989	Interferon (α, β, and ω) receptor 1	−3.1
	PDXK	AW449022	Pyridoxal (pyridoxine, vitamin B6) kinase	−4.0
	HTATIP2	BC002439	HIV-1 Tat interactive protein 2, 30 kDa	−4.1
	CARD10	AY028896	Caspase recruitment domain family, member 10	−4.2
	RAB34	AF322067	RAB34, member RAS oncogene family	−4.7
	GM2A	AL513583	GM2 ganglioside activator protein	−14.6
Cytoskeleton	TPX2	AF098158	TPX2, microtubule-associated protein homolog (*Xenopus laevis*)	−3.8
Enzyme	IDS	BF346014	Iduronate 2-sulfatase (Hunter syndrome)	+3.6
	USP49	NM_004275	Ubiquitin-specific protease 49	−3.9
	ICMT	AL578502	Isoprenylcysteine carboxyl methyltransferase	−4.1

BRCA1 vector, then infected with BRCA1-RNAi adenovirus (Fig. 3 *Bc* and *Bd*). The RNAi-resistant BRCA1 carrying Q356R (Fig. 3*Bc1–3*) mutation rescued the normal acinus formation with the appearance of the central hollow lumen in 1 week of growth. On the other hand, the RNAi-resistant BRCA1 the carrying M1775R mutation (Fig. 3*Bd1–3*) failed to rescue, suggesting that BRCT domain of BRCA1 is important for mediating the acinus formation.

MEC Proliferates in the Absence of Functional BRCA1. Next, to verify whether the loss of the functional BRCA1 leads to the cellular proliferation, cells were recovered from the Matrigel after 1 week of growth, and the number of viable cells was counted (Fig. 3*C*). The populations of cells that formed the normal acinus structures had cell numbers two to three times that originally seeded, suggesting that cells had divided at least once before committing themselves to differentiate, in a manner comparable to adipocyte differentiation mediated by RB (22). On the other hand, the populations that failed to form the acinus structures had cell numbers six to eight times the original, suggesting these cells continued dividing during the course of the experiment. This result reflects the fact that cellular differentiation and proliferation are opposing signaling events (17), and the presence of the functional BRCA1 seems essential for driving cells into the differentiation pathway.

Loss of BRCA1 at the Initial Stage of Acinar Morphogenesis Up-Regulates the Expression of Proliferation but Down-Regulates Differentiation Genes. To assess the differential gene expression pattern caused by the loss of BRCA1 at the initial stage of acinar morphogenesis, we performed pair-wise microarray analyses on MCF10A cells infected with the control luciferase- or BRCA1-siRNA adenovirus and grown in 3D cultures for 15 h (Table 1). The result confirmed that BRCA1-RNAi largely decreased the BRCA1 level (−7.9-fold). In BRCA1-depleted cells, a mammary differentiation factor STAT5B (23) and a caretaker/cancer susceptibility gene FANCA (24), as well several IFN- or caspase-associated proteins, were down-regulated. Concomitantly, in these cells, certain proliferation markers, including HMGA2 (25), angiopoietin-1 (26), and CaM kinase II β (27), were up-regulated. The data suggest that the gene expression pattern of BRCA1-depleted cells at the initial stage of acinar morphogenesis is overall directed toward proliferation rather than differentiation, supporting our phenotypic observation that the BRCA1-depleted MEC failed to enter the acinus-forming pathway but instead proceeded to proliferate.

Conditioned Medium from Differentiating MEC Rescue the Acinus-Forming Phenotype of Differentiation-Defective MEC. Because the transfection efficiency in MCF10A cells usually reach ≈30–50%, it was surprising to observe that cells transfected with wild-type, as well as Q356R point mutant, BRCA1 rescued the acinus formation phenotype (Fig. 3). Then, we speculated that certain factor(s) released from BRCA1-positive cells might have influenced the morphogenesis of the neighboring BRCA1-negative cells. To test this possibility, the conditioned medium collected from MCF10A cells, which has been infected with the luciferase-RNAi/GFP adenovirus, was used to plate and continually (every 15 h) feed BRCA1-RNAi/GFP adenovirus-infected MCF10A cells in 3D culture. In contrast to BRCA1-depleted cells with the fresh growth medium (Fig. 4*Aa1–3*), ≈20% of BRCA1-depleted cells fed with the conditioned medium were able to resume the acinus-forming phenotype (Fig. 4*Ab1–3*). This observation suggests that MCF10A cells secrete certain paracrine/autocrine factor(s) in response to ECM signals, whereas cells depleted of BRCA1 lack such activity.

Next, we tested whether the administration of the conditioned medium from the differentiating MCF10A cells can alter the growth and morphology of breast cancer cells lain in 3D cultures (Fig. 4*B*). Two different breast carcinoma cell lines were tested: HCC1937 (Fig. 4 *Ba* and *Bb*), which expresses a truncated form of BRCA1 at one of the C-terminal BRCT domains (28) and SKBR3 (Fig. 4 *Bc* and *Bd*), which expresses a low basal level of BRCA1 (29). Both cancer cells lain in 3D culture with fresh growth medium formed irregular-shaped large aggregates (Fig. 4 *Ba1–3* and *Bc1–3*). Conversely, when

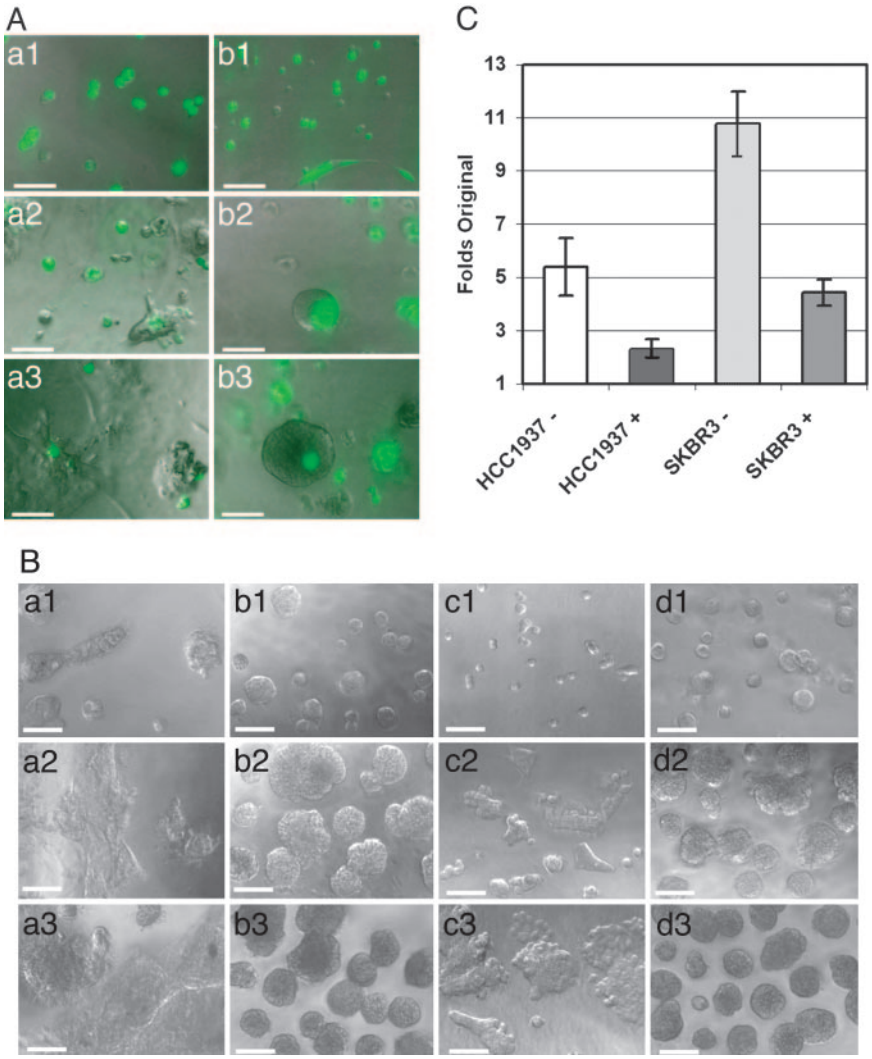

Fig. 4. Conditioned medium from differentiating MEC revert the phenotypes of acinus formation-defective MEC. (*A*) MCF10A cells were infected with 20 moi of adenovirus expressing the control luciferase RNAi or BRCA1 RNAi (*a* and *b*). Cells were fed every 15 h with fresh (*a*) or conditioned medium from the control cells (*b*). Acinar morphogenesis was monitored at different time points [(*1*) 15 h, (*2*) 4 days, and (*3*) 7 days] of growth in 3D culture. (Bar, 50 μm.) (*B*) Breast cancer cells (*a* and *b*, HCC1937; *c* and *d*, SKBR3) were fed every 12 h with fresh growth (*a* and *c*) or conditioned medium from differentiating MCF10A cells (*b* and *d*). Acinar morphogenesis was monitored at different time points [(*1*) 15 h, (*2*) 4 days, and (*3*) 7 days] of growth in 3D culture. (Bar, 50 μm.) (*C*) MEC with different manipulations were recovered from 3D culture after 1 week of growth in the absence (−) or presence (+) of conditioned medium, and the percentage viable cell numbers with respect to that originally plated was calculated.

these cancer cells were continually (every 12 h) fed with the conditioned growth medium from the differentiating MCF10A cells, a large fraction of the cell population (>40%) formed acinus-like spherical structures (Fig. 4 *Bb1–3* and *Bd1–3*) with the appearance of the central hollow lumen in 1 week. In addition, a significant number of dead cells were observed among those incapable of forming an acinus-like structure (≈60%). After 1 week of growth, the number of viable cells was counted (Fig. 4*C*). BRCA1-depleted MCF10A cells were ≈40% lower in those treated with the conditioned medium than untreated. Also, the two cancer cell lines tested were at least 60% lower in those treated with the conditioned medium than untreated. These observations suggest that the differentiating MCF10A cells, in response to ECM signals, secrete certain paracrine/autocrine factors, which promote differentiation for the nonmalignant/malignant MEC that have reduced BRCA1 functions.

Discussion

The processes of mammary acinus formation are comprised of a series of molecular events, including ECM signal response, cell migration/communication, aggregate formation, polarity establishment, and hollow lumen formation by luminal cell death (16–18). Although the completion of the entire cycle may take 2–3 weeks, all of the distinctive stages of acinus formation become evident within 1 week of growth in 3D cultures (16, 18). We took advantage of this rapid approach to study the acinar morphogenesis of MEC after BRCA1 was depleted. Our study shows that the loss of the functional BRCA1 leads to the aberrant acinus formation and enhanced proliferation of MEC. The role of BRCA1 in MEC differentiation manifests from the very early step (<15 h), where cells elongate and establish cell-to-cell communications in response, to the ECM signal, the point of the cell fate decision between differentiation and proliferation (17). MEC defective in this critical step at the initial stage of acinar morphogenesis fail to differentiate despite that the BRCA1 level is expected to gradually recover during the course of the experiment. BRCA1 must sit in a position to mediate the differentiation signals transcending from ECM and then respond to them through regulating the expression of specific genes involved in the very early stage of MEC differ-

entiation. Importantly, this entire signal cascade requires an intact BRCT domain of BRCA1, which interacts with several cellular proteins, including CtIP, HDAC, SWI/SNF, and BACH1 (8, 30, 31), and is worth pursuing.

MEC depleted of BRCA1 fail to enter the differentiation pathway but instead proliferate in 3D culture. This result is at odds with the previous notion that cells lacking BRCA1 will fail to repair damaged DNA and accumulate genetic errors leading to cell death (10). However, certain fractions of BRCA1-depleted cells eventually continue proliferating and form a tumor (10). The 3D culture system may supply the best condition that allows MEC to respond to ECM signals for a decision about proliferation, differentiation, or death. It is possible that a failure to enter the acinus-forming pathway may trigger deregulated cellular proliferation, because cells committed to differentiate will be subjected to regulations on the cell cycle/division to define the organoid's polarity, size, and shape (17), whereas cells defective in this process will be precluded from such regulations. Based on this premise, we observed that in BRCA1-depleted cells, certain proliferation markers, including HMGA2, angiopoietin-1, and CaM kinase II β, were up-regulated, whereas a mammary differentiation factor STAT5B and a caretaker/cancer susceptibility gene FANCA were down-regulated. Nevertheless, it has yet to be examined whether BRCA1 is directly involved in the transcriptional regulations of these genes or whether their expression patterns change as the BRCA1 level gradually recovers during the course of the experiment.

Furthermore, surprisingly, the application of the conditioned medium from differentiating MEC can promote differentiation for the nonmalignant/malignant MEC that have reduced BRCA1 functions. This observation suggests that differentiating MEC, in response to ECM signals, secrete certain paracrine/autocrine factors to induce differentiation of the recipient cells. Several paracrine factors, such as Wnt, EGF, IGF, Rank, and TGF family members, are shown to regulate growth and differentiation of MEC (32, 33). Determination of the factors that can induce differentiation of malignant MEC and their link to the BRCA1 signaling pathway is currently under vigorous investigations.

Taken together, our results suggest BRCA1 is involved in the cellular response to the ECM stimuli that drive MEC into a proper differentiation pathway. Once this initial signaling is disrupted, cells proceed to proliferate. Such consequence may, at least in part, account for the malignancy experienced by BRCA1 mutation carriers as well as sporadic breast cancer in which BRCA1 expression is significantly reduced (4).

We thank Aihua Li and Eva Lee for help in setting up the 3D culture system. This work was supported by a grant from the National Institutes of Health (RO1 CA94170, to W.-H.L.) and a predoctoral fellowship from the Department of Defense (W81XWH-05-1-0322).

1. Miki, Y., Swensen, J., Shattuck-Eidens, D., Futreal, P. A., Harshman, K., Tavigian, S., Lin, Q., Cochran, C., Bennett, L. M., Ding, W., *et al*. (1994) *Science* **266,** 66–71.
2. Couch, F. J., DeShano, M. L., Blackwood, M. A., Calzone, K., Stopfer, J., Campeau, L., Ganguly, A. A., Rebbeck, T. & Weber, B. L. (1997) *N. Engl. J. Med.* **336,** 1409–1415.
3. Zheng, L., Li, S., Boyer, T. G. & Lee, W.-H. (2000) *Oncogene* **19,** 6159–6175.
4. Thompson, M. E., Jensen, R. A., Obermiller, P. S., Page, D. L. & Holt, J. T. (1995) *Nat. Genet.* **9,** 444–450.
5. Ting, N. S. Y. & Lee, W-H. (2004) *DNA Rep.* **3,** 935–944.
6. Deng, C.-X. & Brodie, S. G. (2000) *BioEssays* **22,** 728–737.
7. Zheng, L., Pan, H., Li, S., Flesken-Nikitin, F., Chen P.-L., Boyer, T. G. & Lee, W.-H. (2000) *Mol. Cell* **6,** 757–768.
8. Li, S., Chen, P. L., Subramanian, T., Chinnadurai, G., Tomlinson, G., Osborne, C. K., Sharp, Z. D. & Lee, W.-H. (1999) *J. Biol. Chem.* **274,** 11334–11338.
9. Cantor, S. B., Bell, D. W., Ganesan, S., Kass, E. M., Drapkin, R., Grossman, S., Wahrer, D. C., Sgroi, D. C., Lane, W. S., Haber, D. A., *et al.* (2001) *Cell* **105,** 149–160.
10. Deng, C.-X. & Wang, R.-H. (2003) *Hum. Mol. Genet.* **12,** R113–R123.
11. Shen, S. X., Weaver, Z., Xu, X., Li, C., Weinstein, M., Chen, L., Guan, X. Y., Ried, T. & Deng, C. X. (1998) *Oncogene* **17,** 3115–3124.
12. Tomlinson, G. E., Chen, T. T., Stastny, V. A., Virmani, A. K., Spillman, M. A., Tonk, V., Blum, J. L., Schneider, N. R., Wistuba, I. I., Shay, J. W., *et al.* (1998) *Cancer Res.* **58,** 3237–3242.
13. Brodie, S. G., Xu, X., Qiao, W., Li, W. M., Cao, L. & Deng, C. X. (2001) *Oncogene* **20,** 7514–7523.
14. Rajan, J. V., Wang, M., Marquis, S. T. & Chodosh, L. A. (1996) *Proc. Natl. Acad. Sci. USA* **93,** 13078–13083.
15. Xu, X., Wagner, K. U., Larson, D., Weaver, Z., Li, C., Ried, T., Hennighausen, L., Wynshaw-Boris, A. & Deng, C. X. (1999) *Nat. Genet.* **22,** 37–43.
16. Debnath, J., Muthuswamy, S. K. & Brugge, J. S. (2003) *Methods* **30,** 256–268.
17. Weaver, V. M. & Bissell, M. J. (1999) *J. Mammary Gland Biol. Neoplasia* **4,** 193–201.
18. Debnath, J., Mills, K. R., Collins, N. L., Reginato, M. J., Muthuswamy, S. K. & Brugge, J. S. (2002) *Cell* **111,** 29–40.
19. He, T.-C., Zhou, S., da Costa, L. T., Yu, J., Kinzler, K. W. & Vogelstein, B. (1998) *Proc. Natl. Acad. Sci. USA* **95,** 2509–2514.
20. Sui, G., Soohoo, C., Affar, E. B., Gay, F., Shi, Y., Forrester, W. C. & Shi, Y. (2002) *Proc. Natl. Acad. Sci. USA* **99,** 5515–5520.
21. Zheng, L. & Lee, W.-H. (2001) *Exp. Cell Res.* **264,** 2–18.
22. Chen, C. F., Li, S., Chen, Y., Chen, P. L., Sharp, Z. D. & Lee, W.-H. (1996) *J. Biol. Chem.* **271,** 32863–32868.
23. Liu, X., Robinson, G. W., Gouilleux, F., Groner, B. & Hennighausen, L. (1995) *Proc. Natl. Acad. Sci. USA* **92,** 8831–8835.
24. Folias, A., Matkovic, M., Bruun, D., Reid, S., Hejna, J., Grompe, M., D'Andrea, A. & Moses, R. (2002) *Hum. Mol. Genet.* **11,** 2591–2597.
25. Tessari, M. A., Gostissa, M., Altamura, S., Sgarra, R., Rustighi, A., Salvagno, C., Caretti, G., Imbriano, C., Montovani, R., Del Sal, G., *et al.* (2003) *Mol. Cell. Biol.* **23,** 9104–9116.
26. Caine, G. J., Blann, A. D., Stonelake, P. S., Ryan, P. & Lip, G. Y. (2003) *Eur. J. Clin. Invest.* **33,** 883–890.
27. Kahl, C. R. & Means, A. R. (2003) *Endocr. Rev.* **24,** 719–736.
28. Yu, X., Chini, C. C. S., He, M., Mer, G. & Chen, J. (2003) *Science* **302,** 639–642.
29. Blagosklonny, M. V., An, W. G., Melillo, G. M., Nguyen, P., Trepel, J. B. & Meckers, L. M. (1999) *Oncogene* **18,** 6460–6468.
30. Bochar, D. A., Wang, L., Beniya, H., Kinev, A., Xue, Y., Lane, W. S., Wang, W., Kashanchi, F. & Shiekhattar, R. (2000) *Cell* **102,** 257–265.
31. Yarden, R. I. & Brody, L. C. (1999) *Proc. Natl. Acad. Sci. USA* **96,** 4983–4988.
32. Rosen, J. M. (2003) *Breast Dis.* **18,** 3–9.
33. Serra, R. & Crowley, M. R. (2003) *Breast Dis.* **18,** 61–73.

[Submitted to *Cancer Cell*, March 18, 2006]

Removal of BRCA1/CtIP/ZBRK1 repressor complex on *ANG1* promoter leads to accelerated breast tumor growth contributed by prominent vasculature

Saori Furuta*, Ju-Ming Wang*, Shuanzeng Wei,Yung-Ming Jeng, Xianzhi Jiang, Bingnan Gu, Phang-Lang Chen, Eva Y-H.P. Lee, and Wen-Hwa Lee**

Running title: BRCA1/CtIP/ZBRK1 represses ANG1 expression in mammary epithelial cells

Department of Biological Chemistry, College of Medicine, University of California, Irvine, CA 92697, USA

* These two authors contributed equally to this work.

**Correspondence: whlee@uci.edu; FAX (949) 824-9767

Summary

BRCA1 exerts transcriptional repression through interaction with CtIP in the C-terminal BRCT domain and ZBRK1 in the central domain. A dozen of genes including angiopoietin-1 (*ANG1*), a secreted angiogenic factor, are co-repressed by BRCA1 and CtIP based on microarray analysis of mammary epithelial cells in 3-D culture. BRCA1, CtIP and ZBRK1 form a complex that coordinately represses ANG1 expression via a ZBRK1 recognition site in *ANG1* promoter. Impairment of this complex upregulates ANG1, which stabilizes endothelial capillary structure. Consistently, *Brca1*-deficient mouse breast tumors exhibit accelerated growth, pronounced vascularization and overexpressed ANG1. These results suggest, besides its role in maintaining genomic stability, BRCA1 directly regulates the expression of angiogenic factors to modulate the tumor microenvironment.

Significance

BRCA1 plays an essential role in DNA damage response and cell-cycle checkpoint control. Little is known how an impaired function of BRCA1 is correlated with accelerated growth and progression of hereditary and sporadic breast cancer. We show that BRCA1 forms a repressor complex with CtIP and ZBRK1 at a ZBRK1 responsive element of the angiopoietin-1 promoter in mammary epithelial cells. A defect of this complex formation derepresses ANG1 transcription, promoting the survival and vascular maturation of endothelial cells in a paracrine fashion. This enhanced angiogenesis contributes to exacerbated malignancy of *Brca1*-deficient mouse breast tumors. Thus, our study unveils a mechanism for how BRCA1 modulates the tumor microenvironment by transcriptional regulation.

Introduction

Mutations in the breast cancer susceptibility gene *BRCA1* account for up to 50% of hereditary breast cancer and almost all hereditary breast and ovarian cancer (Couch et al., 1997; Easton et al., 1993). Also, reduced *BRCA1* expression is often correlated with accelerated progression and growth of sporadic breast cancer (Thompson et al., 1995). BRCA1 participates in DNA damage repair, cell-cycle checkpoint control and transcriptional regulation, serving as a tumor suppressor to maintain genomic stability. The *BRCA1* gene encodes a 220 kDa nuclear phosphoprotein of 1863 amino acids (Kim et al., 1996; Miki et al., 1994), characterized by distinctive protein-protein interaction surfaces. The N-terminal RING finger domain dimerizes with BARD1 for ubiquitin ligase activity (Hashizume et al., 2001), while the C-terminus possesses two tandem copies of the BRCT motif that interact with RNA polymerase II holoenzyme (Scully et al., 1997), histone deacetylases (HDAC) (Yarden and Brody, 1999), CBP/p300 (Pao et al., 2000), BACH1 (Yu et al., 2003) and CtIP (Li et al., 1999). The central region, mainly encoded by exon 11, contains two nuclear localization signals (Chen et al., 1995) and interacts with a DNA damage repair complex Rad50/Mre11/NBS1 (Zhong et al., 1999) and transcription repressor ZBRK1 (Zheng et al., 2000).

BRCA1 is also involved in developmental and differentiation processes (Furuta et al., 2005; Lane et al., 1995) and exhibits a temporal and spatial expression pattern. *Brca1* homozygous knockout mice succumb to developmental defects and die during early embryonic stages (E6.5) (Hakem et al., 1996; Liu et al., 1996). In mammary tissue, BRCA1 is upregulated in rapidly dividing, differentiating cells but downregulated in regressing cells (Marquis et al., 1995). BRCA1 facilitates differentiation of mammary epithelia, and its depletion promotes

cellular proliferation (Furuta et al., 2005) while the restoration reverses a neoplastic phenotype (Kumar et al., 1999). Mouse mammary tissue with a conditional *Brca1* knockout displays abnormal ductal morphogenesis and breast tumor (Xu et al., 1999).

BRCA1 confers a transcriptional repression on stress-responsive genes *p21* and *GADD45* through interaction with CtIP at the C-terminal BRCT domain (aa 1651-1863) (Li et al., 1999; Li et al., 2001; Yu et al., 1998). CtIP is an 897 amino-acid protein originally identified as a cofactor of CtBP, a C-terminal binding protein of human adenovirus E1A protein (Boyd et al., 1993; Fusco et al., 1998) involved in transcriptional repression, particularly, during development and oncogenesis (Chinnadurai, 2002). CtIP interacts with different proteins via discrete modules including a PLDLS motif (aa 490-494) for CtBP (Schaeper et al., 1998), a region aa 299-345, phosphorylated at S327, for BRCA1 (Yu and Chen, 2004) and a LECEE motif (aa 153-157) for retinoblastoma (RB) tumor suppressor (Fusco et al., 1998). Certain tumor-linked mutations of the BRCT domain abolish CtIP association and prevent BRCA1-dependent transcriptional repression (Li et al., 1999). Moreover, *Ctip*-null mouse embryos die at E4.0 as blastocysts fail in S phase entry, while the heterozygotes are short-lived and develop various kinds of tumors that retain a single wild-type allele, indicative of haploid insufficiency, suggesting that *Ctip* is a bona fide tumor susceptibility gene (Chen et al., 2005).

Two interacting tumor suppressors, BRCA1 and CtIP, coordinate in certain transcriptional regulatory pathways, namely, DNA damage-response and cell cycle checkpoint control (Li et al., 1999; Li et al., 2001). However, it is largely unknown whether they cooperate in a transcriptional repression beyond the stress-inducible pathways. In the present study, we have identified a dozen of genes co-repressed by BRCA1 and CtIP in MCF10A mammary epithelial cells (MEC) in 3-D culture using microarray analyses. Among them, we have

examined angiopoietin-1 (*ANG1*), a factor secreted to stimulate angiogenesis of neighboring endothelial cells (Suri et al., 1996), for a BRCA1- and CtIP-dependent transcriptional repression. We demonstrate that BRCA1, CtIP and ZBRK1 form a repressor complex at a recognition site of ZBRK1 in *ANG1* promoter and a defect of this repressor complex formation derepresses ANG1 expression in MEC that promotes vascular maturation of the neighboring endothelial cells. Consistently, *Brca1*-deficient mouse breast tumors display a high level of Ang1 expression, prominent vascularization and accelerated growth.

Results

ANG1 expression is co-repressed by BRCA1 and CtIP in MEC

We previously demonstrated that MEC depleted of BRCA1 in 3-D matrix, a close mimicry to the *in vivo* microenvironment, undergo vigorous proliferation but fail in acinar differentiation (Furuta et al., 2005), reflecting a phenotype similar to breast tumorigenesis. Depletion of CtIP evokes a similar phenotype (unpublished data). To identify the genes directly co-regulated by the two proteins during this process, we performed microarray analyses on MCF10A cells depleted of BRCA1 or CtIP by adenoviral RNAi and grown in 3-D culture for 15h. Among over a hundred genes with altered expression profiles, only a dozen were concomitantly upregulated (fold > 2, p <0.05) in both sets of experiments (Table 1), suggesting that they are co-repressed by BRCA1 and CtIP. At least five of them, the upregulations of which were confirmed by RT-PCR (Fig.S1), are proliferation markers including *ANG1*, *bFGF*, *HMGA2*, *LIMK1* and *RFC1* (Caine et al., 2003; Cullmann et al., 1995; Davila et al., 2003; Imura et al., 2004; Tessari et al., 2003). We were particularly intrigued by *ANG1*, a secreted angiogenic

factor modulating the tumor microenvironment. ANG1 promotes tubular formation and survival of endothelial cells and enhances blood vessel growth and maturation upon binding to Tie2 receptor tyrosine kinase on the endothelial cell surface (Hayes et al., 1999; Kwak et al., 1999; Suri et al., 1996). Dysfunction of BRCA1 is correlated with accelerated growth and progression of breast tumors (Stoppa-Lyonnet et al., 2000; Xu et al., 1999), often displaying microvascular proliferation (Goffin et al., 2003). Consistently, we observed that *Brca1*-deficient mouse breast tumors exhibit pronounced growth and extensive mature vascularization (Table 2).

To verify our microarray data showing that a decrease of BRCA1 (-7.9 fold) or CtIP (-3.9 fold) in MCF10A cells evoked a significant increase of ANG1 (+2.7 or +2.4 fold, respectively) (Fig.1A,B), we performed RT-PCR on MCF10A cells in 3-D culture. Reduced expression of BRCA1 or CtIP paralleled increased ANG1 expression (Fig.1C,D), suggesting that a deficiency of either BRCA1 or CtIP upregulates ANG1 expression.

The interaction between BRCA1 and CtIP is required for transcriptional repression of the ANG1 promoter

BRCA1 and CtIP both serve as transcriptional co-repressors and interact with each other. To determine a potential transcriptional regulation of ANG1 by BRCA1 and CtIP, we measured the luciferase reporter activity of *ANG1* promoter constructs with different lengths (Fig.2A) after BRCA1 or CtIP was depleted in MCF10A cells by adenoviral RNAi. Only construct C, encoding a 3 kb-full length *ANG1* promoter, showed a significant increase in the activity as BRCA1 level decreased by increasing adenoviral RNAi (Fig.2B,C), suggesting that the region –3040 to –1799 is essential for transcriptional repression by BRCA1. Similar results were obtained in both 2-D monolayer and 3-D cultures, independent of the experimental systems. Likewise, as CtIP was

depleted by adenoviral RNAi, construct C showed a comparable increase in the activity (Fig.2D). These results imply that the region (–3040/–1799) of *ANG1* promoter is subject to co-repression by BRCA1 and CtIP.

To test if the interaction of BRCA1 and CtIP is required for ANG1 repression, we generated RNAi-resistant BRCA1 and CtIP expression plasmids which are either wild-type or point mutants: C61G (RING domain), Q356R (central region) and M1775R (BRCT domain) for BRCA1; and S327A for CtIP. BRCA1 (M1175R) mutation impairs binding of a group of BRCT domain-interacting proteins including CtIP, whereas CtIP (S327A) mutation impedes BRCA1 binding (Yu and Chen, 2004; Yu et al., 1998). Treatment of MCF10A cells with an RNAi-resistant BRCA1 (Fig.2E) or CtIP (Fig.2F) plasmid prior to the cognate adenoviral RNAi infection effectively rescued their expressions. As the luciferase activity of construct C was measured under this context (Fig.2G), cells expressing RNAi-resistant wild-type BRCA1 or CtIP endured the repression despite the increasing adenoviral RNAi. In contrast, cells expressing RNAi-resistant BRCA1 (M1775R) or CtIP (S327A) mutant failed to repress the activity even at the lowest dose (5 MOI) of adenoviral infection, suggesting that the interaction of BRCA1 and CtIP is essential for repressing ANG1 transcription. Interestingly, BRCA1 (Q356R) mutant, but not BRCA1 (C61G) mutant, also failed to repress ANG1 transcription, indicating that the central region of BRCA1 is also involved in this process.

A single ZBRK1 recognition site in *ANG1* promoter mediates BRCA1 and CtIP co-repression

BRCA1, lacking intrinsic sequence-specific DNA binding activity, interacts at the central region (aa 341-748) with ZBRK1, which mediates BRCA1-dependent transcriptional repression

of certain genes by directly binding to a consensus motif (GGGxxxCAGxxxTTT) (Zheng et al., 2000). If a ZBRK1 recognition site is indeed present in *ANG1* promoter, a chimeric tranactivator, a ZBRK1 DNA binding domain fused to a VP16 transactivation domain, would recognize this sequence and upregulate the *ANG1* promoter activity (Zheng et al., 2000). As shown in Fig.3A, the presence of this chimeric ZBRK1 promoted the luciferase reporter activity of construct C, but not A or B, suggesting that the region –3040 to –1799 contains potential ZBRK1 recognition sites involved in transcriptional repression of ANG1 by ZBRK1. Sequence analyses revealed that this region contains a total of five potential ZBRK1 binding sites. To map a functional ZBRK1 binding site, we generated deletion mutants in the first three ZBRK1 binding sites (C1: Δ–2600/-2200), the last two sites (C2: Δ–2200/-1800) and all the five sites (C3: Δ–2600/-1800) (Fig.3B). Reporter assays showed that C1 and C3, but not C2, were repression-defective and neither BRCA1- (Fig.3C) nor CtIP-depletion (Fig.3D) further derepressed the activities. Sequence analysis of the first three potential sites revealed a nearly canonical ZBRK1 consensus motif (-2310/-2296: GAGxxxCAGxxxTTT). We then generated a mutant construct C-mt-Z, by substituting the five essential nucleotides (GTTxxTTTGxxxTTT) (Fig.3B) and found that this mutant responded to repression by neither BRCA1 (Fig.3C), CtIP (Fig.3D) nor ZBRK1 (Fig.3A), suggesting that this putative site (-2310/-2296) is a strong candidate for a ZBRK1 binding site.

To test whether ZBRK1 directly binds to this putative site, a 33-mer radiolabeled oligonucleotide probe (-2319/-2287) harboring the ZBRK1 recognition site (-2310/-2296) of *ANG1* promoter (wt-Z) was used to perform EMSA using either GST-fused ZBRK1 eight-Zn finger domain (Zheng et al., 2000) or nuclear extract. We included a non-labeled wt- (wt-Z) or point mutant ZBRK1 (mt-Z) binding sequence of *ANG1* promoter and AP12, a canonical consensus ZBRK1 binding sequence (Zheng et al., 2000) for competition experiments. As

expected, a non-labeled wild-type *ANG1* or AP12 competitor, but not mutant *ANG1*, competed with a labeled wild-type probe for binding ZBRK1, suggesting that ZBRK1 directly binds to this site (-2310/-2296) (Fig.3E). To further demonstrate that this ZBRK1 recognition site is functional in vivo, we generated a heterologous reporter construct with a 800-bp fragment (-2600/-1800) containing a wild-type (3P-26-wt-Z) or mutant (3P-26-wt-Z) ZBRK1 binding site (-2310/-2296) (Fig.3F). Reporter assay showed that the activity increased as ZBRK1 level decreased by increasing adenoviral ZBRK1 RNAi (see below Fig.4A), whereas a mutant ZBRK1 site was repression-defective (Fig.3F), further confirming that this site is an authentic ZBRK1 recognition site.

ZBRK1, BRCA1 and CtIP form a repressor complex on *ANG1* promoter

Since BRCA1/CtIP co-represses *ANG1* promoter via a ZBRK1 recognition site, it is expected that depletion of ZBRK1 would derepress *ANG1* expression, similar to that of BRCA1 and CtIP depletion (Fig.1A). To test this possibility, we depleted ZBRK1 by adenoviral mediated RNAi in MCF10A cells in 3-D culture and assessed the ANG1 expression level using RT-PCR. Reduced ZBRK1 expression paralleled increased ANG1 expression (Fig.4A), suggesting that a deficiency of ZBRK1 upregulates *ANG1* repression. These results altogether implicate that ZBRK1, BRCA1 and CtIP coordinately repress *ANG1* expression. Since BRCA1 binds CtIP via its BRCT domain (Li et al., 1999) and ZBRK1 via central domain (Zheng et al., 2000), it is likely that these three proteins form a repressor complex on the ZBRK1 recognition site. To test this possibility, these three proteins were reciprocally co-immunoprecipitated from nuclear extract (Fig.4B), suggesting that they form a complex. Next, we mixed a radiolabeled

oligonucleotide probe containing a wild-type (wt-Z or AP12) or mutant (mt-Z) ZBRK1 binding sequence with nuclear extract for immunoprecipitation. Antibodies against ZBRK1, BRCA1 as well as CtIP brought down a wild-type (wt-Z or AP12), but not mutant (mt-Z), oligonucleotide specifically (Fig.4C). Finally, to demonstrate that this complex is associated with *ANG1* promoter *in vivo*, we performed ChIP assay on a 300 bp fragment around the ZBRK1 site (-2400/-2100). As shown in Fig.4D, ZBRK1, BRCA1 and CtIP co-localized on *ANG1* promoter, while an individual depletion of either protein by RNAi completely abolished the association of all the three proteins with the promoter, suggesting that the three participants are all essential for the complex formation. Taken together, these data substantiate that BRCA1, CtIP and ZBRK1 coordinately form a repressor complex tethered at the ZBRK1 recognition site in *ANG1* promoter.

Expression of ANG1 from MEC is essential for the stability of capillary structure formed by neighboring endothelial cells in 3-D matrix

To assess a biological consequence of derepressed ANG1 expression, we co-cultured MCF10A cells with human umbilical endothelial cells (HUVEC) in 3-D matrix. HUVEC alone formed a thin layer of capillary structure in a day but soon came to disintegrate and died in a week under this experimental condition (Fig.5B.a). When HUVEC were co-cultured with luciferase-RNAi treated MCF10A cells, they formed a well-defined thin layer of capillary structure in a day; however, the endothelial cells, indicated as non-fluorescent cells, started to die in 3 days and the capillary structure disintegrated in a week (Fig.5B.b). When HUVEC unlabeled (Fig.5B.e) or labeled with GFP-histone H2B (Fig.5B.f) were co-cultured with MCF10A/ANG1

cells that stably express ANG1 by retroviral infection (Fig.5A), they formed a thick layer of capillary structure, which sustained over a week. When HUVEC were co-cultured with MCF10A cells depleted of BRCA1 (Fig.5B.c) or CtIP (Fig.5B.d), they formed a thick layer of capillary structure, which maintained for a week in a manner similar to those co-cultured with MCF10A/ANG1 cells. To validate the essential role of ANG1 in the survival of co-cultured endothelial cells, we treated MCF10A cells with ANG1 siRNA, which was shown by western analysis to completely deplete ANG1 in MCF10A/ANG1 cells after 36h (Fig.5C). HUVEC co-cultured with ANG1 siRNA-treated MCF10A/ANG1 cells formed a thin layer of capillary structure in a day but soon came to disintegrate and died after a week (Fig.5D.h) in a manner similar to those co-cultured with Luc-RNAi infected MCF10A cells (Fig.5D.a,b). Likewise, when HUVEC were co-cultured with MCF10A cells treated with ANG1 siRNA prior to BRCA1- (Fig.5D.d) or CtIP-RNAi (Fig.5D.f) infection, they formed a thin layer of capillary structure in a day, but the endothelial cells, indicated as non-fluorescent cells, started to disintegrate after 3 days and died in a week, leaving aggregates of fluorescent MEC. Based on these observations, upregulated expression of ANG1 from MEC, either by the overexpression construct or by depletion of BRCA1 or CtIP, is essential for the stability of capillary structure formed by the co-cultured endothelial cells in 3-D matrix.

Brca1-deficient mouse breast tumors exhibit an accelerated growth and harbor enlarged blood vessels along with up-regulated Ang1 expression

To test if these *in vitro* observations gain supports from animal studies, we examined breast tumor samples from *Brca1*-deficient mice. *BRCA1*-associated tumorigenesis is often

linked to a loss of *p53* (Xu et al., 1999). To recapitulate the *BRCA1*-related tumor pathogenesis, we used a mouse model inactivated in both *Brca1* and *p53* genes ($Brca1^{\Delta 11/\Delta 11};p53^{\Delta 5\text{-}6/\Delta 5\text{-}6}$) (n = 17) in comparison to mice inactivated only in *p53* gene ($p53^{\Delta 5\text{-}6/\Delta 5\text{-}6}$) (n = 14) as a control (Lin et al., 2004; Xu et al., 1999). *Brca1*-deficient tumors exhibited a substantially shorter latency than control tumors (6.1 ±1.3 vs. 18.3 ±2.2 months) to reach a comparable size (0.996 ±0.460 vs. 1.072 ±0.588 ml, respectively) (Table 2). In general, *Brca1*-deficient tumors displayed an ensanguined appearance, noticeably distinct from control tumors with the same size (Fig.6A). To examine the blood vessel status of these tumor specimens, they were stained against CD31, an endothelial cell marker (Machein et al., 2004). Apparently, *Brca1*-deficient tumors contained larger blood vessels compared to control tumors (Fig.6B,C). The blood vessel luminal area of *Brca1*-deficient tumor was almost three times the size of control tumor (224.2 ±135.0 vs. 82.8 ±33.9 μm^2, $p < 0.001$) (Table 2) while microvascular density (/mm^2) did not significantly differ between the two sets of tumors ($p = 0.22$, data not shown), consistent with a finding that ANG1 causes vessel enlargement without angiogenic sprouting during development (Thurston et al., 2005). Interestingly, analogous regulatory elements including a ZBRK1 recognition site were found in the mouse *Ang1* promoter region (Fig.6D), suggesting that mouse Ang1 expression may be subjected to a similar mode of regulation as human. Consistently, Ang1 expression was mostly upregulated in *Brca1*-deficient tumors, but not in control tumors (Fig.6E). Taken together, these results support a notion that inactivation of *BRCA1* in MEC upregulates ANG1 expression to stabilize blood vessel maturation from neighboring endothelial cells.

Discussion

BRCA1 plays an essential role in DNA damage response and cell-cycle checkpoint control which are intimately linked to a restraint of cancer initiation. Additional functions of BRCA1 remain to be further characterized. In this communication, we revealed that BRCA1, in coordination with CtIP and ZBRK1, exerts a transcriptional repression on ANG1 that pertains to cancer progression. To mimic *in vivo* conditions, we depleted BRCA1 and CtIP in normal MEC cultured in extracellular matrix. Microarray analyses identified a dozen of genes co-repressed by BRCA1 and CtIP. We focused on *ANG1* since it may participate in cancer progression through angiogenesis. Our results demonstrated that BRCA1 and CtIP, along with ZBRK1, form a repressor complex on *ANG1* promoter via a ZBRK1 recognition element (Fig.6F) and that *Brca1*-deficient mouse breast tumors exhibit prominent vascularization and accelerated growth along with Ang1 upregulation. This suggests that derepressed ANG1 expression in MEC in the absence of BRCA1 is a pathogenic drive for neoplastic growth.

Depletion of BRCA1 impairs acinar differentiation but promotes proliferation of MEC into a tumor-like aggregate in 3-D culture (Furuta et al., 2005). Strikingly, our preliminary results showed that depletion of CtIP as well as ZBRK1 leads to a phenotype identical to BRCA1-depletion, suggesting that they share at least one common regulation pathway. ZBRK1, a sequence-specific transcriptional repressor that binds to the canonical GGGxxxCAGxxxTTT motif, interacts with the central region of BRCA1 (aa 341-748) and mediates the transcriptional repression activity of BRCA1 (Zheng et al., 2000). Interestingly, there are five potential ZBRK1 sites in *ANG1* promoter due to the degeneracy of the consensus motif, but only one site (nt –2310/-2296) has the *in cis* transcriptional repression function since point mutations at this site abolished the capacity (Fig.3). Through this recognition site, ZBRK1, BRCA1 and CtIP form a

repressor complex on *ANG1* promoter. This conclusion was supported by the following observations. First, a defect in BRCA1, CtIP and ZBRK1 complex formation on *ANG1* promoter, caused by lacking one of the participants or their interactions, impairs ANG1 transcriptional repression. Second, BRCA1, CtIP and ZBRK1 can be co-immunoprecipitated with an oligonucleotide containing the wild-type ZBRK1 recognition sequence. Third, by ChIP analysis, BRCA1, CtIP and ZBRK1 co-localized at *ANG1* promoter. It is noted that depletion of one of these three components leads to disassembly of the entire repressor complex including ZBRK1, suggesting that the stability of ZBRK1 binding to the recognition site depends on the integrity of the complex. This is partly consistent with a previous finding that BRCA1 facilitates ZBRK1 binding to the recognition site *in vivo* (Tan et al., 2004).

Apparently, the regulation of *ANG1* promoter would be more complicated than that by a repressor complex alone. Since a point mutation in the ZBRK1 binding site (-2310/-2296) as well as a deletion in the surrounding region (Δ-2600/-1800) upregulated ANG1 transcription (Fig.3), the region –2310 to –2296 must be involved in repression while the region outside (-3040/-2600) in activation once the repression is removed. It is probable that derepression of ANG1 in the region –2310/-2296 evokes a subsequent activation of the neighboring region by altering the local chromatin structure to allow the accessibility to certain transactivators. In fact, the region around the ZBRK1 binding site in *ANG1* promoter encompasses various conserved transcriptional regulatory elements such as AML1 (CBF-α/CBFA2) (Fig.6D) which is responsible for upregulation of ANG1 expression during embryogenesis (Brown et al., 2004; Takakura et al., 2000). Clearly, derepression is the first step for full activation of the promoter. How these two steps are coordinated in regulating *ANG1* promoter warrants further investigation.

Angiogenesis is a critical process for tumor progression. ANG1 promotes tubular formation and survival of endothelial cells (Hayes et al., 1999; Kwak et al., 1999) and enhances blood vessel growth and maturation (Suri et al., 1996). Consistently, we observed that ANG1 expressed from MEC exerts a paracrine action on neighboring endothelial cells for their survival and stability of capillary structures. *Brca1*$^{\Delta 11/\Delta 11}$;*p53*$^{\Delta 5\text{-}6/\Delta 5\text{-}6}$ mouse breast tumors, characterized by their accelerated growth and ensanguined appearance, harbor prominently enlarged blood vessels compared to *p53*$^{\Delta 5\text{-}6/\Delta 5\text{-}6}$ mouse breast tumors. Such a phenotype of *Brca1*-deficient breast tumors may be attributed to derepressed ANG1 expression from MEC, stabilizing the adjacent blood vessels and promoting their growth and maturation to provide conduits for supplying nutrition, consistent with the observation that ANG1 causes vessel enlargement without angiogenic sprouting during development (Thurston et al., 2005). Furthermore, gliomas overexpressing ANG1 exhibit accelerated tumor growth and extensive mature vascular network allowing for better tumor perfusion (Machein et al., 2004) in a manner similar to *Brca1*$^{\Delta 11/\Delta 11}$;*p53*$^{\Delta 5\text{-}6/\Delta 5\text{-}6}$ mouse breast tumors. Although it is yet to be examined whether *BRCA1*-associated human breast tumors harbor enlarged blood vessels as seen in mice, these tumors metastasize to a distant site through the blood stream instead of lymphatic routes (Foulkes et al., 2003), suggesting that they develop blood vessels much earlier than non-*BRCA1*-associated tumors. Our observation in mice provides a likely explanation to this clinical manifestation.

In addition to *ANG1*, one of the identified genes *bFGF* is also involved in angiogenesis (Imura et al., 2004), while several other genes, *HMGA2*, *LIMK1* and *RFC1*, are involved in proliferation (Cullmann et al., 1995; Davila et al., 2003; Tessari et al., 2003). As the net effect, an impaired transcriptional repression activity of BRCA1 and CtIP will promote angiogenic and proliferative potentials of cells. Currently, we are examining if the remaining genes are regulated

under a similar mechanism as *ANG1*, aiming to further understand the cellular events involved in the progression of *BRCA1*- and *CtIP*-associated tumors.

A neoplastic potential due to a dysfunction of BRCA1 tumor suppressor has been largely ascribed to the genomic instability resulting from defects in DNA damage-responsive pathways. However, the present study shows that BRCA1-deficiency modulates the tissue microenvironment by derepression of ANG1 (or bFGF) that promotes the growth of adjacent vasculature in a paracrine fashion to nourish a neoplasm. Moreover, an aberrant activity of a BRCA1-interacting partner, CtIP tumor suppressor, also deregulates ANG1 expression, which may likewise pertain to the etiology of tumor growth in *Ctip* heterozygous mice (Chen et al., 2005). Apparently, these two tumor suppressors have much broader activities than other tumor susceptibility genes, such as MSH2 and ATM, which exclusively play roles in guarding genomic stability. This study concludes that BRCA1 and CtIP possess an additional role in tumor suppression, via a ZBRK1 element, by regulating the intercellular signaling within the tissue microenvironment besides maintaining the genomic stability within the cell. This view will extend their tumor suppression functions to the surroundings that influence the fate of neighboring cells and fortify the pathogenic relevance of their defect to neoplastic growth.

Experimental procedures

Cell cultures

Human mammary epithelial MCF10A cells and umbilical endothelial cells (HUVEC) were cultured as described (Debnath et al., 2003; Shekhar et al., 2000), respectively.

denoviral RNAi construction

The adenovirus-based RNAi vector was generated by cloning an expression cassette of U6 promoter-BRCA1, -CtIP or -ZBRK1 short hairpin RNAi (0.4 kb) into pAdTrack plasmid upstream of a CMV-GFP cassette (1.6 kb) (He et al., 1998; Sui et al., 2002). The target sequences are BRCA1: 5'-GGCTACAGAAACCGTGCCAAA-3'; CtIP: 5'-GGGAGCAGACCTTTCTCAGTA-3'; and ZBRK1: 5'-AAACCATGTCATGAACATGAT-3'. Adnoviruses were produced as described (Furuta et al., 2005). MCF10A cells seeded at $5x10^5$ cells/60mm plate were infected with adenovirus at a designated MOI for 24h.

RNAi-resistant BRCA1and CtIP plasmids

The RNAi-targeted nucleotide sequence in a full-length BRCA1 cDNA, the expression of which was driven by a CMV promoter in CHpL vector (Li et al., 1999), was partially substituted without affecting the amino acid residues (5'-GGCTACCGGAATAGGGCCAAA-3'), and a cancer-linked point mutation of BRCA1 (C61G, Q356R or M1775R) was introduced into the

wild-type RNAi-resistant construct using a site-directed mutagenesis kit (Stratagene). Similarly, the RNAi-targeted nucleotide sequence in GFP-CtIP construct, containing a full length CtIP cDNA N-terminally fused to GFP (Li et al., 2001), was partially substituted as (5'-GGGAGCTGACTTGTCTCAGTA-3'), and a point mutation of CtIP (S327A) was introduced into the wild-type RNAi-resistant construct. Correct substitutions were confirmed by sequencing. Respective primer sequences used are shown in Table S1. MCF10A cells seeded at $5x10^5$ cells/60mm plate were transfected with 3μg of RNAi-resistant construct using Fugene6 (Roche) prior to adenoviral RNAi infection.

Microarray and RT-PCR

MCF10A cells seeded at $5x10^5$ cells/60mm plate were infected with adenoviral luciferase-, BRCA1-, CtIP- or ZBRK1-RNAi in duplicate at 20 MOI for 24h. Infected cells were re-seeded at $5x10^5$ cells in a 60mm plate pre-coated with Growth Factor Reduced Matrigel (BD Biosciences) and covered with the growth medium containing 2% Matrigel at 37°C for 15h. RNA was extracted from these cells with Trizol (Invitrogen), clarified by RNeasy spin column (Quiagen) and quality assessed. cDNA synthesized from the harvested RNA using SuperScript Double-Stranded cDNA Synthesis Kit (Invitrogen) served as a template for PCR amplification with respective primers (Table S1), and a portion of it was biotin-labeled using GeneChip® IVT Labeling Kit (Affymetrix), hybridized onto Affymetrix HG U133 PLUS 2.0 array (54,676 genes) and stained with streptavidin-phycoerythrin. The hybridized array was analyzed using GeneChip® Scanner 3000 and GCOS 1.2 software (Affymetrix) for multiplex pair-wise comparison at the UCI Microarray Core service. The statistical significance was evaluated by

ANOVA single factor analysis using MS Excel XP, and the fold-difference >2 as well as *p*-value <0.05 was considered significant.

Luciferase reporter assay

ANG1 promoter constructs A (-821/+199), B (-1799/+199) and C (-3040/+199) that regulate luciferase expression in pGL2 vector were from Peter Oettgen (Harvard Institutes of Medicine, MA)(Brown et al., 2004). Construct C was subjected to site-directed mutagenesis (Stratagene) to generate deletions of ZBRK1 binding sites: C1 (Δ-2600/-2200), C2 (Δ-1200/-1800) and C3 (Δ-2600/-1800); point mutations in a putative ZBRK1 site (-2310/-2296): C-mt-Z; and a fragment containing ZBRK1 binding sites (-2600/-1800): 3P-26-(wt/mt)-Z with respective primers (Table S1). Correct changes were confirmed by sequencing and restriction digestion. MCF10A cells seeded at $5x10^5$ cells/60mm plate were transfected with 3μg of luciferase reporter and 0.5μg of β-galactosidase plasmids using Fugene6 prior to adenoviral RNAi infection. Luciferase and β-galactosidase reporter activities were measured using a reporter assay kit (Promega).

Electromobility shift assay (EMSA)

EMSA was performed as described (Zheng et al., 2000). A γ-^{32}P-ATP labeled oligonucleotide probe (6000cpm) harboring a ZBRK1 site (-2310/-2296) in *ANG1* promoter (wt-Z, -2319/-2287) was incubated with 50ng of GST-ZBRK1-Zn protein purified from *E. coli* or 8μg of MCF10A nuclear extract of in 40μl of DNA binding buffer containing 1μg of poly(dI-dC) at room temperature. For competition experiment, molar excess of an unlabeled wild-type or mutant

oligonucleotide was included. The sense oligonucleotides used are wild-type ZBRK1 site in *ANG1* promoter (wt-Z): 5'-ACACACGTG**GAG**GAA**CAG**ATT**TTT**AACAGTCTC-3'; a point mutant of the ZBRK1 site in *ANG1* promoter (mt-Z): 5'-ACACACGTGGTTGATTTGATTTTTAACAGTCTC-3'; and a canonical ZBRK1 binding sequence (AP12) (Zheng et al., 2000): 5'-GATCCAC**GGG**ACG**CAG**GTG**TTT**TGTGCCG-3' (ZBRK1 recognition motifs are shown in bold). The reaction was resolved on 5% native polyacrylamide gel at 4°C and autoradiographed.

DNA immunoprecipitation

DNA immunoprecipitation was performed as described (Zheng et al., 2000). A radiolabeled oligonucleotide of wt-Z, mt-Z or AP12, was incubated with 50μg of nuclear extract in 200μl of DNA binding buffer containing 1μg of poly(dI-dC) at room temperature for 30 min. The protein-oligonucleotide complex was precipitated by protein G sepharose beads loaded with a respective antibody and resolved on 5% polyacrylamide gel followed by autoradiography.

Immunoprecipitation

1μg of antibody against HA (Ctrl), CtIP, BRCA1 or ZBRK1 was added to 200μg of pre-clarified MCF10A nuclear extract and incubated at 4ºC overnight. Antibody-protein complex was precipitated by protein G-sepharose beads and washed with TEN buffer (10mM Tris-HCl (pH8.0), 0.25mM EDTA, 50mM NaCl). Immunoprecipitates were resolved on 8% SDS-PAGE and detected by western analysis.

Chromatin immunoprecipitation (ChIP)

ChIP assay was performed as described (Saccani et al., 2001) with a minor modification. Chromatins from 1% formaldehyde-treated MCF10A cells were sonicated to ~500 bp fragments and immunoprecipitated with antibodies against HA, ZBRK1, BRCA1 and CtIP at 4°C overnight. Chromatin-antibody complexes were washed with buffer 1 (0.1% SDS, 0.5% Triton X-100, 2mM EDTA, 20mM Tris-HCl (pH8.0), 150mM NaCl), buffer 2 (0.1% SDS, 2mM EDTA, 20mM Tris-HCl (pH8.0), 500mM NaCl) then TE buffer (10mM Tris-HCl (pH8.0), 1mM EDTA). After reversal of cross-linking, immunoprecipitated chromatin was subjected to PCR reaction for a 300 bp fragment (–2400/-2100) of *ANG1* promoter around a ZBRK1 binding site with respective primers (Table S1).

ANG1 retrovirus and siRNA

A full length of ANG1 cDNA, KIAA0003 clone (GenBank NO. D13628), was from Takahiro Nagase (Kazusa DNA Research Institute, Chiba, Japan) (Nomura et al., 1994). A 1.7 kb coding sequence fragment was obtained by PCR reaction with respective primers (Table S1) and cloned into pQCXIH vector (BD Biosciences). GP_2-293 packaging cells were transfected with pQCXIH/ANG1 and pVSVG plasmids using Lipofectin, and retrovirus was harvested in the conditioned medium. MCF10A cells were infected with retrovirus using 8μg/ml polybrene, and the stable clones (MCF10A/ANG1) were selected with 70μg/ml Hygromycin B (Roche). Overexpression of ANG1 was confirmed by western analysis using a rabbit anti-ANG1 antibody

(1:500, Alpha Diagnostic). ANG1 siRNA was synthesized against the target sequence: 5'-AAGGCTTGGTTACTCGTCAAA-3' (Qiagen). MCF10A cells seeded at $5x10^5$ cells/60mm plate were transfected with 400pmol of ANG1 or luciferase siRNA for 24h using Oligofectamine (Invitrogen) prior to adenoviral infection.

3-D co-culture

$5x10^4$ MCF10A cells and $5x10^4$ HUVEC were seeded together into each well of 8-well chamber slide coated with Matrigel and covered with SFM supplemented with EGF and bFGF (Shekhar et al., 2000). Fluorescence imaging was performed with Phase I/FITC filters on a Zeiss Axiovert 200M equipped with Hamamatsu Photonics K.K. Deep Cooled Digital Camera using Axiovision 4.4 software.

Immunohistochemistry

Animal experiments were performed under federal guidelines and approved by Institutional Animal Care and Use Committee at UCI. Mice with *p53* gene floxed at exons 5-6 (*p53fp/fp*) were generated as described (Lin et al., 2004). Mice with *Brca1* gene floxed at exon 11 (*Brca1f11/f11*) were from Chu-Xia Deng (NIH) (Xu et al., 1999). Both strains were crossed to obtain *Brca1f11/f11;p53fp/fp* mice. *p53fp/fp* or *Brca1f11/f11;p53fp/fp* mice were crossed with *Wap-Cre* mice and genotyped to obtain $p53^{\Delta 5\text{-}6/\Delta 5\text{-}6}$ or $Brca1^{\Delta 11/\Delta 11}; p53^{\Delta 5\text{-}6/\Delta 5\text{-}6}$ strain, respectively. Dissected mouse breast tumors were fixed in 4% paraformaldehyde overnight. 4-5μm sections were deparaffinized, hydrated and digested in 0.05% trypsin at 37°C. After blocked with 3%

H_2O_2 and non-immune horse serum, sections were incubated at room temperature with a rabbit anti-mouse CD31 antibody and link antibodies, followed by peroxidase-conjugated streptavidin complex and diaminobenzidine tetrahydroxychloride solution as the peroxidase substrate (Vector Laboratories). The sections were counterstained with hematoxylin. Photomicrographs were taken with Zeiss Axioplan 2 Imaging and Axion Vision 4.4 Software. Tumor vessel count, vessel areas, and the mean vessel area per 200X field were calculated. The statistical significance was evaluated by Student *t*-test using MS Excel XP.

Acknowledgements

We thank Drs. Peter Oettgen (Harvard Institutes of Medicine, MA) for *ANG1* reporter constructs, Christopher Hughes (UCI) for HUVEC, Takahiro Nagase (Kazusa DNA Research Institute, Chiba, Japan) for KIAA0003 clone, Chu-Xia Deng (NIH) for *Brca1*-floxed mice and Eric Wang, Christopher Smith and Suh-Chin J. Lin for various assistances. This work was supported by grants from the National Institutes of Health (RO1 CA94170 to W-HL; R37 CA049649 to EL), a predoctoral fellowship from the Department of Defense (W81XWH-05-1-0322 to SF) and a physician scientist award from the National Health Research Institute in Taiwan to Y-MJ.

References

Boyd, J. M., Subramanian, T., Schaeper, U., La Regina, M., Bayley, S., and Chinnadurai, G. (1993). A region in the C-terminus of adenovirus 2/5 E1a protein is required for association with a cellular phosphoprotein and important for the negative modulation of T24-ras mediated transformation, tumorigenesis and metastasis. EMBO J *12*, 469-478.

Brown, C., Gaspar, J., Pettit, A., Lee, R., Gu, X., Wang, H., Manning, C., Voland, C., Goldring, S. R., Goldring, M. B., Libermann, T.A.*, et al.* (2004). ESE-1 is a novel transcriptional mediator of angiopoietin-1 expression in the setting of inflammation. J Biol Chem *279*, 12794-12803.

Caine, G. J., Blann, A. D., Stonelake, P. S., Ryan, P., and Lip, G. Y. H. (2003). Plasma angiopoietin-1, angiopoietin-2 and Tie-2 in breast and prostate cancer: a comparison with VEGF and Flt-1. Eur J Clin Invest *33*, 883-890.

Chen, P. L., Liu, F., Cai, S., Lin, X., Li, A., Chen, Y., Gu, B., Lee, E.-H. P., and Lee, W.-H. (2005). Inactivation of CtIP leads to early embryonic lethality mediated by G1 restraint and to tumorigenesis by haploid insufficiency. Mol Cell Biol *25*, 3535-3542.

Chen, Y., Chen, C. F., Riley, D. J., Allred, D. C., Chen, P. L., Von Hoff, D., Osborne, C. K., and Lee, W. H. (1995). Aberrant subcellular localization of BRCA1 in breast cancer. Science *270*, 1424.

Chinnadurai, G. (2002). CtBP family proteins: more than transcriptional corepressors. BioEssays *25*, 9-12.

Couch, F. J., DeShano, M. L., Blackwood, M. A., Calzone, K., Stopfer, J., Campeau, L., Ganguly, A., Rebbeck, T., and Weber, B. L. (1997). BRCA1 mutations in women attending clinics that evaluate the risk of breast cancer. N Engl J Med *336*, 1409-1415.

Cullmann, G., Fien, K., Kobayashi, R., and Stillman, B. (1995). Characterization of the five replication factor C genes of Saccharomyces cerevisiae. Mol Cell Biol *15*, 4661-4671.

Davila, M., Frost, A. R., Grizzle, W. E., and Chakrabarti, R. (2003). LIM kinase 1 is essential for the invasive growth of prostate epithelial cells: implications in prostate cancer. J Biol Chem *278*, 36868-36875.

Debnath, J., Muthuswamy, S. K., and Brugge, J. S. (2003). Morphogenesis and oncogenesis of MCF-10A mammary epithelial acini grown in three-dimensional basement membrane cultures. Methods *30*, 256-268.

Easton, D. F., Bishop, D. T., Ford, D., and Crockford, G. P. (1993). Genetic linkage analysis in familial breast and ovarian cancer: results from 214 families. The Breast Cancer Linkage Consortium. Am J Hum Genet *52*, 678-701.

Foulkes, W. D., Metcalfe, K., Hanna, W., Lynch, H. T., Ghadirian, P., Tunng, N., Olopade, O., Weber, B. L., McLennan, J., Olivotto, I. A.*, et al.* (2003). Disruption of the expected positive correlation between breast tumor size and lymph node status in BRCA1-related breast carcinoma. Cancer *98*, 1569-1577.

Furuta, S., Jiang, X., Gu, B., Cheng, E., Chen, P. L., and Lee, W. H. (2005). Depletion of BRCA1 impairs differentiation but enhances proliferation of mammary epithelial cells. Proc Natl Acad Sci USA *102*, 9176-9181.

Fusco, C., Reymond, A., and Zervos, A. S. (1998). Molecular cloning and characterization of a novel retinoblastoma-binding protein. Genomics *51*, 351-358.

Goffin, J. R., Straume, O., Chappuis, P. O., Brunet, J.-S., Bégin, L. R., Hamel, N., Wong, N., Akslen, L. A., and Foulkes, W. D. (2003). Glomeruloid microvascular proliferation is associated

with p53 expression, germline BRCA1 mutations and an adverse outcome following breast cancer. Br J Cancer *89*, 1031-1034.

Hakem, R., de la Pompa, J. L., Sirard, C., Mo, R., Woo, M., Hakem, A., Wakeham, A., Potter, J., Reitmair, A., Billia, F*., et al.* (1996). The tumor suppressor gene Brca1 is required for embryonic cellular proliferation in the mouse. Cell *85*, 1009-1023.

Hashizume, R., Fukuda, M., Maeda, I., Nishikawa, H., Oyake, D., Yabuki, Y., Ogata, H., and Ohta, T. (2001). The RING heterodimer BRCA1-BARD1 is a ubiquitin ligase inactivated by a breast cancer-derived mutation. J Biol Chem *276*, 14537-14540.

Hayes, A. J., Huang, W. Q., Mallah, J., Yang, D., Lippman, M. E., and Li, L. Y. (1999). Angiopoietin-1 and its receptor Tie-2 participate in the regulation of capillary-like tubule formation and survival of endothelial cells. Microvasc Res *58*, 224-237.

He, T.-C., Zhou, S., da Costa, L. T., Yu, J., Kinzler, K. W., and Vogelstein, B. (1998). A simplified system for generating recombinant adenoviruses. Proc Natl Acad Sci U S A *95*, 2509-2514.

Imura, S., Miyake, H., Izumi, K., Iashiro, S., and Uehara, H. (2004). Correlation of vascular endothelial cell proliferation with microvessel density and expression of vascular endothelial growth factor and basic fibroblast growth factor in hepatocellular carcinoma. J Med Inv *51*, 202-209.

Kim, S. S., Chen, Y. M., O'Leary, E., Witzgall, R., Vidal, M., and Bonventre, J. V. (1996). A novel member of the RING finger family, KRIP-1, associates with the KRAB-A transcriptional repressor domain of zinc finger proteins. Proc Natl Acad Sci USA *93*, 15299-15304.

Kumar, A., Knott, C., Kuus-Reichel, K., and Saedi, M. S. (1999). BRCA1 partially reverses the transforming activity of the ras oncogene. Neoplasia *1*, 417-423.

Kwak, H. J., So, J. N., Lee, S. J., Kim, I., and Koh, G. Y. (1999). Angiopoietin-1 is an apoptosis survival factor for endothelial cells. FEBS Lett *448*, 249-253.

Lane, T. F., Deng, C., Elson, A., Lyu, M. S., Kozak, C. A., and Leder, P. (1995). Expression of Brca1 is associated with terminal differentiation of ectodermally and mesodermally derived tissues in mice. Genes Dev *9*, 2712-2722.

Li, S., Chen, P. L., Subramanian, T., Chinnadurai, G., Tomlinson, G., Osborne, C. K., Sharp, Z. D., and Lee, W.-H. (1999). Binding of CtIP to the BRCT repeats of BRCA1 involved in the transcription regulation of p21 is disrupted upon DNA damage. J Biol Chem *274*, 11334-11338.

Li, S., Ting, N. S. Y., Zheng, L., Chen, P. L., Zlv, Y., Shlloh, Y., Lee, E.-H. P., and Lee, W.-H. (2001). Functional link of BRCA1 and ataxia telangiectasia gene product in DNA damage response. Nature *406*, 210-215.

Lin, S. C., Lee, K. F., Nikitin, A. Y., Hilsenbeck, S. G., Cardiff, R. D., Li, A., Kang, K. W., Frank, S. A., Lee, W.-H., and Lee, E. Y. (2004). Somatic mutation of p53 leads to estrogen receptor alpha-positive and -negative mouse mammary tumors with high frequency of metastasis. Cancer Res *64*, 3525-3532.

Liu, C. Y., Flesken-Nikitin, A., Li, S., Zeng, Y., and Lee, W. H. (1996). Inactivation of the mouse Brca1 gene leads to failure in the morphogenesis of the egg cylinder in early postimplantation development. Genes Dev *10*, 1835-1843.

Machein, M. R., Knedla, A., Knoth, R., Wagner, S., Neuschl, E., and Plate, K. H. (2004). Angiopoietin-1 promotes tumor angiogenesis in a rat glioma model. Am J Pathol *165*, 1557-1570.

Marquis, S. T., Rajan, J. V., Wynshaw-Boris, A., Xu, J., Yin, G. Y., Abel, K. J., Weber, B. L., and Chodosh, L. A. (1995). The developmental pattern of Brca1 expression implies a role in differentiation of the breast and other tissues. Nat Genet *11*, 17-26.

Miki, Y., Swensen, J., Shattuck-Eidens, D., Futreal, P. A., Harshman, K., Tavtigian, S., Liu, Q., Cochran, C., Bennett, L. M., Ding, W., and al., e. (1994). A strong candidate for the breast and ovarian cancer susceptibility gene BRCA1. Science *266*, 66-71.

Nomura, N., Miyajima, N., Sazuka, T., Tanaka, A., Kawarabayasi, Y., Sato, S., Nagase, T., Seki, N., Ishikawa, K., and Tabata, S. (1994). Prediction of the coding sequences of unidentified human genes. DNA Res *1*, 27-35.

Pao, G. M., Janknecht, R., Ruffner, H., Hunter, T., and Verma, I. M. (2000). CBP/p300 interact with and function as transcriptional coactivators of BRCA1. Proc Natl Acad Sci USA *97*, 1020-1025.

Saccani, S., Pantano, S., and Natoli, G. (2001). Two waves of nuclear factor B recruitment to target promoters. J Exp Med *193*, 1351-1359.

Schaeper, U., Subramanian, T., Lim, L., Boyd, J. M., and Chinnadurai, G. (1998). Interaction between a cellular protein that binds to the C-terminal region of adenovirus E1A (CtBP) and a novel cellular protein is disrupted by E1A through a conserved PLDLS motif. J Biol Chem *273*, 8549-8952.

Scully, R., Anderson, S. F., Chao, D. M., Wei, W., Ye, L., Young, R. A., Livingston, D. M., and Parvin, J. D. (1997). BRCA1 is a component of the RNA polymerase II holoenzyme. Proc Natl Acad Sci USA *94*, 5605-5610.

Shekhar, M. P. V., Werdell, J., and Tait, L. (2000). Interaction with endothelial cells is a prerequisite for branching ductal-alveolar morphogenesis and hyperplasia of preneoplastic human breast epithelial cells: regulation by estrogen. Cancer Res *60*, 439-449.

Stoppa-Lyonnet, D., Ansquer, Y., Dreyfus, H., Gautier, C., Gauthier-Villars, M., Bourstyn, E., Clough, K. B., Magdelenat, H., Pouillart, P., Vincent-Salomon, A.*, et al.* (2000). Familial invasive breast cancers: worse outcome related to BRCA1 mutations. J Clin Oncol *18*, 4053-4059.

Sui, G., Soohoo, C., Affar el, B., Gay, F., Shi, Y., Forrester, W. C., and Shi, Y. (2002). A DNA vector-based RNAi technology to suppress gene expression in mammalian cells. Proc Natl Acad Sci USA *99*, 5515-5520.

Suri, C., Jones, P. F., Patan, S., Bartunkova, S., Maisonpierre, P. C., Davis, S., Sato, T. N., and Yancopoulos, G. D. (1996). Requisite role of angiopoietin-1, a ligand for the TIE2 receptor, during embryonic angiogenesis. Cell *87*, 1171-1180.

Takakura, N., Watanabe, T., Suenobu, S., Yamada, Y., Noda, T., Ito, Y., Satake, M., and Suda, T. (2000). A role for hematopoietic stem cells in promoting angiogenesis. Cell *102*, 199-209.

Tan, W., Zheng, L., Lee, W. H., and Boyer, T. G. (2004). Functional dissection of transcription factor ZBRK1 reveals zinc fingers with dual roles in DNA-binding and BRCA1-dependent transcriptional repression. J Biol Chem *279*, 6576-6587.

Tessari, M. A., Gostissa, M., Altamura, S., Sgarra, R., Rustighi, A., Salvagno, C., Caretti, G., Imbriano, C., Mantovani, R., Del Sal, G.*, et al.* (2003). Transcriptional activation of the cyclin A gene by the architectural transcription factor HMGA2. Mol Cell Biol *23*, 9104-9116.

Thompson, M. E., Jensen, R. A., Obermiller, P. S., Page, D. L., and Holt, J. T. (1995). Decreased expression of BRCA1 accelerates growth and is often present during sporadic breast cancer progression. Nat Genet *9*, 444-450.

Thurston, G., Wang, Q., Baffert, F., Rudge, J., Papadopoulos, N., Jean-Guillaume, D., Wiegand, S., Yancopoulos, G. D., and McDonald, D. M. (2005). Angiopoietin 1 causes vessel enlargement, without angiogenic sprouting, during a critical developmental period. Development *132*, 3317-3326.

Xu, X., Wagner, K. U., Larson, D., Weaver, Z., Li, C., Ried, T., Hennighausen, L., Wynshaw-Boris, A., and Deng, C. X. (1999). Conditional mutation of Brca1 in mammary epithelial cells results in blunted ductal morphogenesis and tumour formation. Nat Genet *22*, 37-43.

Yarden, R. I., and Brody, L. C. (1999). BRCA1 interacts with components of the histone deacetylase complex. Proc Natl Acad Sci USA *96*, 4983-4988.

Yu, X., and Chen, J. (2004). DNA damage-induced cell cycle checkpoint control requires CtIP, a phosphorylation-dependent binding partner of BRCA1 C-terminal domains. Mol Cell Biol *24*, 9478-9486.

Yu, X., Chini, C. C., He, M., Mer, G., Chen, J., Yu, X., Chini, C. C., He, M., Mer, G., and Chen, J. (2003). The BRCT domain is a phospho-protein binding domain. Science *302*, 639-642.

Yu, X., Wu, L. C., Bowcock, A. M., Aronheim, A., and Baer, R. (1998). The C-terminal (BRCT) domains of BRCA1 interact in vivo with CtIP, a protein implicated in the CtBP pathway of transcriptional repression. J Biol Chem *273*, 25388-25392.

Zheng, L., Pan, H., Li, S., Flesken-Nikitin, A., Chen, P. L., Boyer, T. G., and Lee, W. H. (2000). Sequence-specific transcriptional corepressor function for BRCA1 through a novel zinc finger protein, ZBRK1. Mol Cell *6*, 757-768.

Zhong, Q., Chen, C. F., Li, S., Chen, Y., Wang, C. C., Xiao, J., Chen, P. L., Sharp, Z. D., and Lee, W.-H. (1999). Association of BRCA1 with the hRad50-hMre11-p95 complex and the DNA damage response. Science *285*, 747-750.

Figure legends

Figure 1. ANG1 is co-repressed by BRCA1 and CtIP in MCF10A cells

A: Microarray data of relative expression levels of BRCA1 and ANG1 in MCF10A cells infected with adenoviral BRCA1- vs. luciferase-RNAi at 20 MOI for 24h and grown in 3-D culture for 15h.

B: Microarray data of relative expression levels of CtIP and ANG1 in MCF10A cells infected with adenoviral CtIP- vs. luciferase-RNAi at 20 MOI for 24h and grown in 3-D culture for 15h.

C: RT-PCR analysis on BRCA1 and ANG1 expressions in MCF10A cells infected with adenoviral luciferase- or BRCA1-RNAi for 24h and grown in 3-D culture for 15h. α-tubulin (α-TUB) serves as a loading control.

D: RT-PCR analysis on CtIP and ANG1 expressions in MCF10A cells infected with adenoviral luciferase- or CtIP-RNAi for 24h and grown in 3-D culture for 15h. α-tubulin serves as a loading control.

Figure 2. Interaction of BRCA1 and CtIP is required for transcriptional repression of *ANG1* promoter

A: Schematics of *ANG1* reporter constructs A-C in the promoter region. A: –821/+199; B: –1799/+199; and C: –3040/+199 from the start codon.

B: Relative luciferase activity of reporter constructs A-C in MCF10A cells infected with adenoviral BRCA1-RNAi for 24h in 2-D monolayer culture.

C: Relative luciferase activity of reporter constructs A-C in MCF10A cells infected with adenoviral BRCA1-RNAi for 24h in 3-D culture.

D: Relative luciferase activity of reporter constructs A-C in MCF10A cells infected with adenoviral CtIP-RNAi for 24h in 2-D monolayer culture.

E: Western analysis on the expression of BRCA1 (wt, C61G, Q356R or M1775R) after treated with an RNAi-resistant (RM) construct prior to adenoviral BRCA1-RNAi infection. p84 serves as a loading control.

F: Western analysis on the expression of GFP-CtIP (wt or S327A) after treated with an RNAi-resistant (RM) construct prior to adenoviral CtIP-RNAi infection. p84 serves as a loading control.

G: Relative luciferase activity of reporter construct C in MCF10A cells treated with an RNAi-resistant BRCA1 (wt, C61G, Q356R or M1775R) or CtIP (wt or S327A) prior to the cognate adenoviral RNAi infection (BR: BRCA1, CT: CtIP).

Figure 3. BRCA1, CtIP and ZBRK1 co-repress ANG1 expression via a single ZBRK1 recognition element in the promoter

A: Relative luciferase activity of *ANG1* reporter constructs A-C and C-mt-Z, a point mutant in a putative ZBRK1 binding site (-2310/-2296), in MCF10A cells expressing a chimeric (CM) ZBRK1 where KRAB repression domain is replaced with VP16 activation domain.

B: Schematics of *ANG1* reporter constructs derived from construct C. C-wt: wild-type (-3040/+199) containing five potential ZBRK1 binding sites; C-mt-Z: a point mutant in a putative ZBRK1 binding site (-2310/-2296); C1: a deletion of the first three binding sites (Δ-2600/-2200); C2: a deletion of the last two binding sites (Δ-1200/-1800); and C3: a deletion of all the five binding sites (Δ-2600/-1800).

C: Relative luciferase activity of reporter construct C derivatives in MCF10A cells after infected with adenoviral BRCA1-RNAi for 24h.

D: Relative luciferase activity of reporter construct C derivatives in MCF10A cells after infected with adenoviral CtIP-RNAi for 24h.

E: EMSA on a competition between a radiolabeled wild-type ZBRK1 site (-2310/-2296) in *ANG1* promoter (wt-Z, 33 mer) and a non-labeled competitor for binding GST-ZBRK1-Zn protein (the eight-zinc finger domain) or ZBRK1 in nuclear extract (NE). The competitors used are wild-type (wt-Z) or a point mutant (mt-Z) of a ZBRK1 site (-2310/-2296) in *ANG1* promoter (33 mer) and a canonical ZBRK1 binding sequence (AP12, 29 mer).

F: (Top) Relative luciferase activity of a regulatory region (-2600/-1800) in *ANG1* promoter with a wild-type (3P-26-wt-Z) or point mutant (3P-26-wt-Z) of a putative ZBRK1 binding site (-2310/-2296) in MCF10A cells after infected with adenoviral ZBRK1-RNAi for 24h. (Bottom) Schematics of *ANG1* reporter constructs used. 3P-26-wt-Z: a fragment composed of a regulatory

region; and 3P-26-mt-Z: a fragment of a regulatory region with point mutations in a ZBRK1 binding site.

Figure 4. ZBRK1, BRCA1 and CtIP form a repressor complex on *ANG1* promoter

A: RT-PCR analysis on ZBRK1 and ANG1 expressions in MCF10A cells infected with adenoviral luciferase- or ZBRK1-RNAi for 24h and grown in 3-D culture for 15h. β-actin serves as a loading control.

B: Reciprocal co-immunoprecipitation of CtIP, BRCA1 and ZBRK1 from nuclear extract.

C: DNA immunoprecipitation by antibodies against ZBRK1, BRCA1 and CtIP from nuclear extract mixed with an oligonucleotide probe encompassing a ZBRK1 binding sequence (wt-Z, mt-Z, or AP12).

D: ChIP analysis on a 300 bp fragment around a ZBRK1 binding site in *ANG1* promoter (-2400/-2100) to detect the association of BRCA1, CtIP and ZBRK1 in MCF10A cells infected with adenoviral luciferase-, BRCA1-, CtIP- or ZBRK1-RNAi at 20 MOI for 24h.

Figure 5. Expression of ANG1 from MEC is essential for the survival of HUVEC and stability of the capillary structure in 3-D matrix

A: Western analysis on ANG1 expression in MCF10A/ANG1 cells in comparison to the parental MCF10A cells.

B: Survival of HUVEC and stability of the capillary structure in 3-D matrix. Images were captured with Phase I/FITC reflector at 100X magnification. a. HUVEC only; b. HUVEC co-cultured with adenoviral luciferase-RNAi-infected MCF10A cells; c. HUVEC co-cultured with adenoviral BRCA1-RNAi-infected MCF10A cells; d. HUVEC co-cultured with adenoviral CtIP-RNAi-infected MCF10A cells; e. HUVEC co-cultured with MCF10A/ANG1 cells; and f. HUVEC marked for histone H2B and co-cultured with MCF10A ANG1 cells. 1. 24h, 2. 3 days, and 3. 7 days of growth in 3-D culture. Adenoviral RNAi infection was performed at 20 MOI for 24 h. Scale bar: 50μm.

C: Western analysis on ANG1 expression in MCF10A/ANG1 cells treated with luciferase or ANG1 siRNA for a different period of time.

D: Pretreatment of MCF10A cells with ANG1 siRNA destabilizes the capillary structure formed by HUVEC in 3-D matrix. Images were captured with Phase I/FITC reflector at 100X magnification. a,b. HUVEC co-cultured with MCF10A cells pretreated with luciferase (a) or ANG1 (b) siRNA prior to adenoviral luciferase-RNAi infection at 20 MOI for 24h; c,d. MCF10A cells pretreated with luciferase (c) or ANG1 (d) siRNA prior to adenoviral BRCA1-RNAi infection at 20 MOI for 24h; e,f. MCF10A cells pretreated with luciferase (e) or ANG1 (f) siRNA prior to adenoviral CtIP-RNAi infection at 20 MOI for 24h; g,h. HUVEC co-cultured with MCF10A/ANG1 cells pretreated with luciferase (a) or ANG1 (b) siRNA. 1. 24h, 2. 3 days,

and 3. 7 days of growth in 3-D culture. Adenoviral RNAi infection was performed at 20 MOI for 24 h. Scale bar: 50μm.

Figure 6. *Brca1*-deficient mouse breast tumors exhibit enlarged blood vessels and overexpressed ANG1

A: Whole breast tumors (~1.8cm in diameter) excised from (a) $p53^{\Delta 5\text{-}6/\Delta 5\text{-}6}$ and (b) $Brca1^{\Delta 11/\Delta 11}$;$p53^{\Delta 5\text{-}6/\Delta 5\text{-}6}$ mice.

B: Breast tumor sections from $p53^{\Delta 5\text{-}6/\Delta 5\text{-}6}$ mice stained for CD31 (brown) and counterstained with hematoxylin. Mouse ID: (a) 9268, (b) 9342, (c) 9345 and (d) 9349. 1. Image captured at 200X; 2. at 1000X magnification. Scale bar: 50μm.

C: Breast tumor sections from $Brca1^{\Delta 11/\Delta 11}$;$p53^{\Delta 5\text{-}6/\Delta 5\text{-}6}$ mice stained for CD31 (brown) and counterstained with hematoxylin. Mouse ID: (a) 741, (b) 820, (c) 824 and (d) 905. 1. Image captured at 200X; 2. at 1000X. Scale bar: 50μm.

D: *ANG1* promoter region in (a) human and (b) mouse around a ZBRK1 binding site with conserved transcriptional regulatory elements. AML-1: acute myeloid leukemia protein-1; AP-1: activator protein-1; ETS-1: v-ets erythroblastosis virus E26 oncogene homolog 1; IK-1/2: Ikaros 1/2; NF-κB: nuclear factor kappa B.

E: Ang1 expression in $p53^{\Delta 5\text{-}6/\Delta 5\text{-}6}$ and $Brca1^{\Delta 11/\Delta 11}$; $p53^{\Delta 5\text{-}6/\Delta 5\text{-}6}$ mouse breast tumors detected by RT-PCR. GAPDH serves as an internal control.

F: A schematic for ANG1 transcriptional repression by BRCA1, CtIP and ZBRK1 via a ZBRK1 recognition site in the promoter.

Tables

Table 1. Genes co-repressed by BRCA1 and CtIP in 3-D cultured MCF10A cells

Gene Symbol	Gene Name	BRCA1-KD		CtIP-KD	
		Fold	*p*-value	Fold	*p*-value
ACTR1A	ARP1 actin-related protein 1 homolog A, centractin alpha	+ 2.08	0.048	+2.09	0.047
ANG1*	Angiopoietin 1	+2.69	0.016	+2.18	0.026
DCP2	Decapping enzyme hDcp2	+2.19	0.027	+2.09	0.011
DRLM	Down-regulated in liver malignancy	+2.10	0.001	+2.00	0.008
FGF2*	Fibroblast growth factor 2 (basic; bFGF)	+2.03	0.048	+2.04	0.008
HMGA2*	High mobility group AT-hook 2	+4.55	0.002	+2.55	0.001
IL1R1	Interleukin 1 receptor, type I	+2.02	0.004	+2.09	0.001
LIMK1*	LIM domain kinase 1	+2.12	0.049	+2.06	0.005
RFC1*	Replication factor C (activator 1) 1, 145kDa	+2.07	0.047	+2.07	0.027
SLC16A4	Solute carrier family 16 (monocarboxylic acid transporters), member 4	+2.63	0.002	+2.21	0.037
TA-KRP	T-cell activation kelch repeat protein	+2.17	0.048	+2.17	0.009

*Confirmed by RT-PCR (Fig. S1).

Table 2. Blood vessel area of *p53*$^{\Delta 5\text{-}6/\Delta 5\text{-}6}$ and *Brca1*$^{\Delta 11/\Delta 11}$;*p53*$^{\Delta 5\text{-}6/\Delta 5\text{-}6}$ mouse breast tumors

Genotype	Mouse ID	Tumor Vol.[1] (ml)	Latency (Mo.)	Blood Vessel Luminal Area[2] (μm^2)
p53$^{\Delta 5\text{-}6/\Delta 5\text{-}6}$ (n = 14)	9108	1.767	16.5	93.0 (±58.6)
	9128	0.666	18.0	84.5 (±55.8)
	9133	0.762	16.5	66.2 (±39.4)
	9207	0.635	15.0	62.4 (±32.1)
	9268	0.831	21.2	41.0 (±15.6)
	9270	0.831	16.4	49.8 (±15.8)
	9288	0.606	17.3	59.4 (±28.2)
	9311	0.697	19.2	69.1 (±31.1)
	9323	0.762	16.2	94.0 (±54.8)
	9326	0.762	17.1	90.0 (±40.3)
	9339	1.888	21.4	164.4 (±88.9)
	9342	2.145	21.5	141.2 (±95.5)
	9345	2.145	20.5	79.5 (±60.1)
	9349	0.635	19.0	64.1 (±36.2)
	MEAN	1.072	18.3	82.8*
	STDEV	±0.588	±2.2	±33.9
Brca1$^{\Delta 11/\Delta 11}$;*p53*$^{\Delta 5\text{-}6/\Delta 5\text{-}6}$ (n = 17)	**741**	1.767	3.9	329.8 (±209.2)
	806	0.831	8.2	161.3 (±81.2)
	820	2.424	6.5	313.4 (±226.4)
	824	1.337	6.2	310.8 (±75.1)
	847	0.831	6.4	160.3 (±39.9)
	876	0.762	6.4	381.2 (±131.6)
	905	0.905	6.9	139.4 (±95.1)
	913	1.437	6.9	157.6 (±76.3)
	942	0.905	7.1	90.3 (±21.7)
	945	1.064	6.5	111.2 (±38.4)
	947	0.905	3.4	206.7 (±90.5)
	960	0.697	5.9	126.0 (±64.5)
	986	0.762	4.9	182.4 (±63.7)
	1043	0.831	4.4	582.3 (±309.1)
	1094	0.697	6.8	102.2 (±41.3)
	1114	0.831	6.9	95.4 (±43.6)
	1133	0.762	6.4	361.0 (±32.6)
	MEAN	0.996	6.1	224.2*
	STDEV	±0.460	±1.3	±135.0

[1]Tumor Volume = $\pi/6[(L+W+D)/3]^3$
[2]Average luminal area of blood vessels (n = 400) for each tumor sample (±SD)
* *p*-value = 0.000672
Tumor samples used for photographic display (Fig. 5) are indicated in bold

Figures

Figure 1.

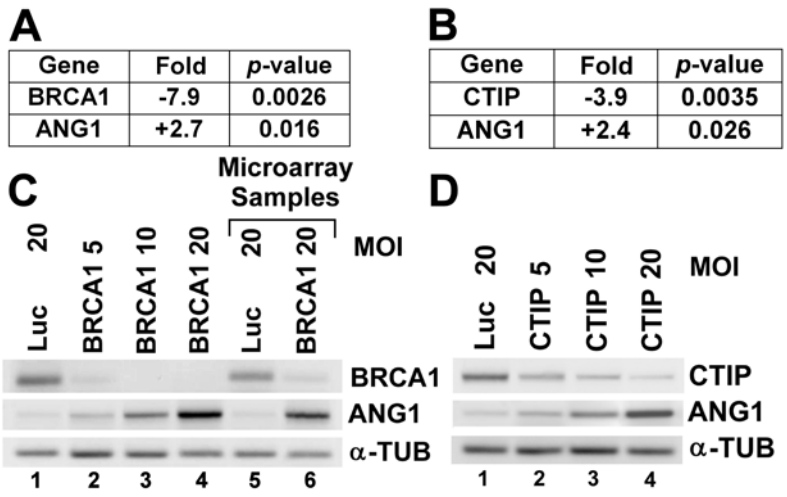

Figure 2.

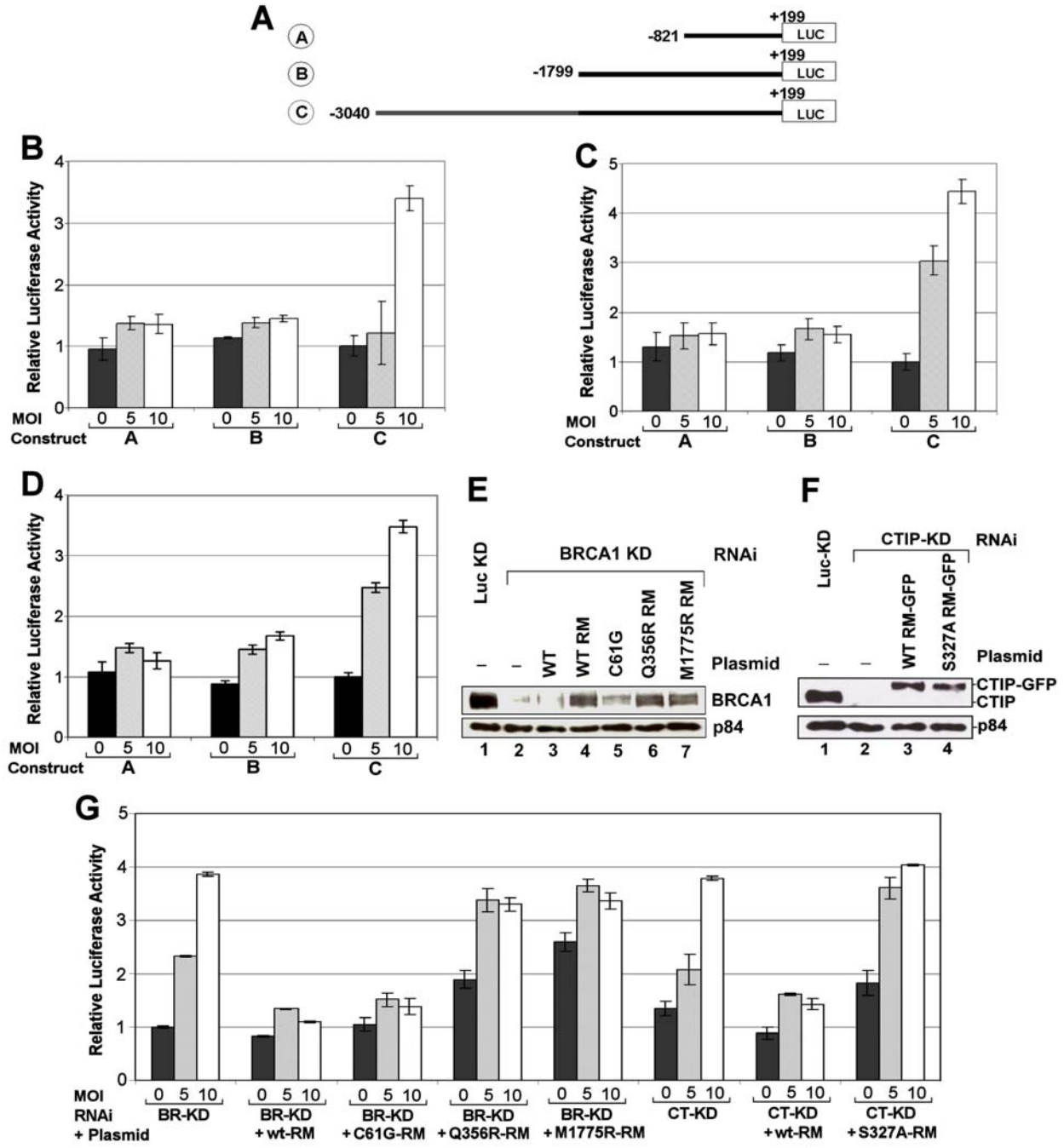
A
A
B
C
-821
-1799
-3040
+199
LUC
B
C
D
Relative Luciferase Activity
MOI
Construct
0 5 10
A
B
C
E
Luc KD
BRCA1 KD
RNAi
Plasmid
–
WT
WT RM
C61G
Q356R RM
M1775R RM
BRCA1
p84
1 2 3 4 5 6 7
F
Luc-KD
CTIP-KD
WT RM-GFP
S327A RM-GFP
CTIP-GFP
CTIP
1 2 3 4
G
RNAi
+ Plasmid
BR-KD
BR-KD + wt-RM
BR-KD + C61G-RM
BR-KD + Q356R-RM
BR-KD + M1775R-RM
CT-KD
CT-KD + wt-RM
CT-KD + S327A-RM

Figure 3.

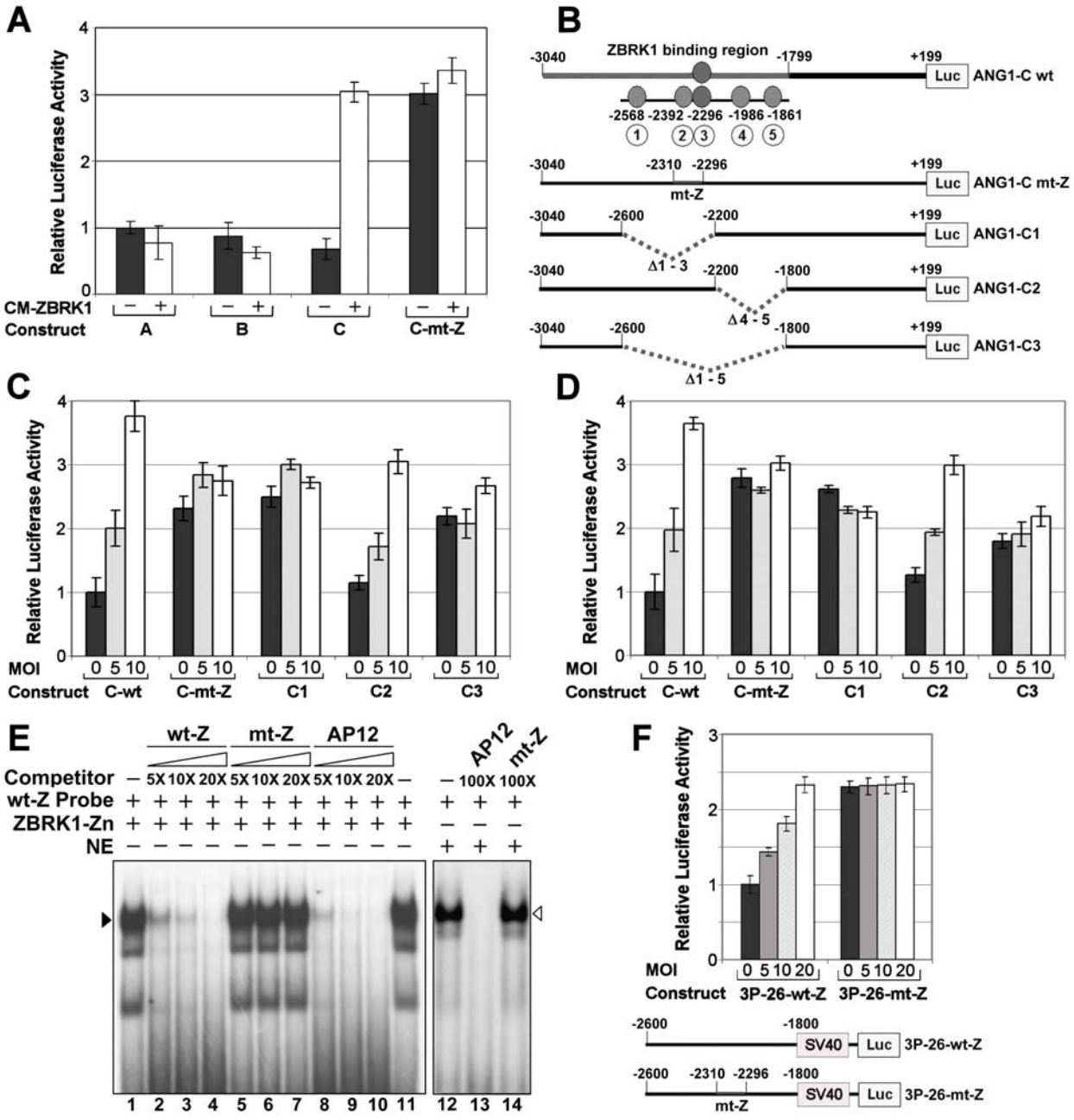
A
Relative Luciferase Activity
CM-ZBRK1
Construct
A
B
C
C-mt-Z
B
ZBRK1 binding region
-3040
-1799
+199
Luc
ANG1-C wt
-2568 -2392 -2296 -1986 -1861
1 2 3 4 5
-2310 -2296
mt-Z
ANG1-C mt-Z
-2600
-2200
ANG1-C1
Δ1 - 3
-1800
ANG1-C2
Δ4 - 5
ANG1-C3
Δ1 - 5
C
D
MOI
0 5 10
C-wt
C-mt-Z
C1
C2
C3
E
wt-Z
mt-Z
AP12
Competitor
5X 10X 20X
100X
wt-Z Probe
ZBRK1-Zn
NE
1 2 3 4 5 6 7 8 9 10 11 12 13 14
F
0 5 10 20
3P-26-wt-Z
3P-26-mt-Z
SV40
Luc

Figure 4.

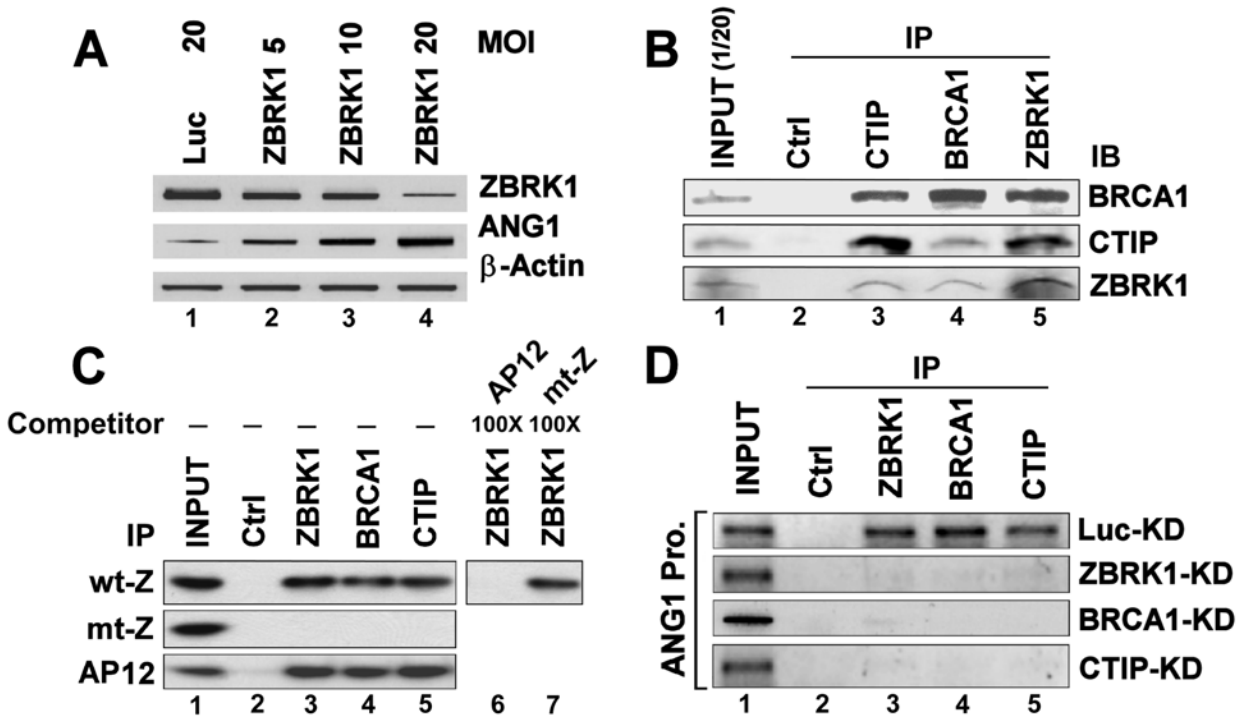
A
MOI
Luc
20
ZBRK1 5
ZBRK1 10
ZBRK1 20
ZBRK1
ANG1
β-Actin
1 2 3 4
B
IP
INPUT (1/20)
Ctrl
CTIP
BRCA1
ZBRK1
IB
BRCA1
CTIP
ZBRK1
1 2 3 4 5
C
AP12
mt-Z
Competitor – – – – – 100X 100X
IP
INPUT
Ctrl
ZBRK1
BRCA1
CTIP
ZBRK1
ZBRK1
wt-Z
mt-Z
AP12
1 2 3 4 5 6 7
D
IP
INPUT
Ctrl
ZBRK1
BRCA1
CTIP
ANG1 Pro.
Luc-KD
ZBRK1-KD
BRCA1-KD
CTIP-KD
1 2 3 4 5

Figure 5.

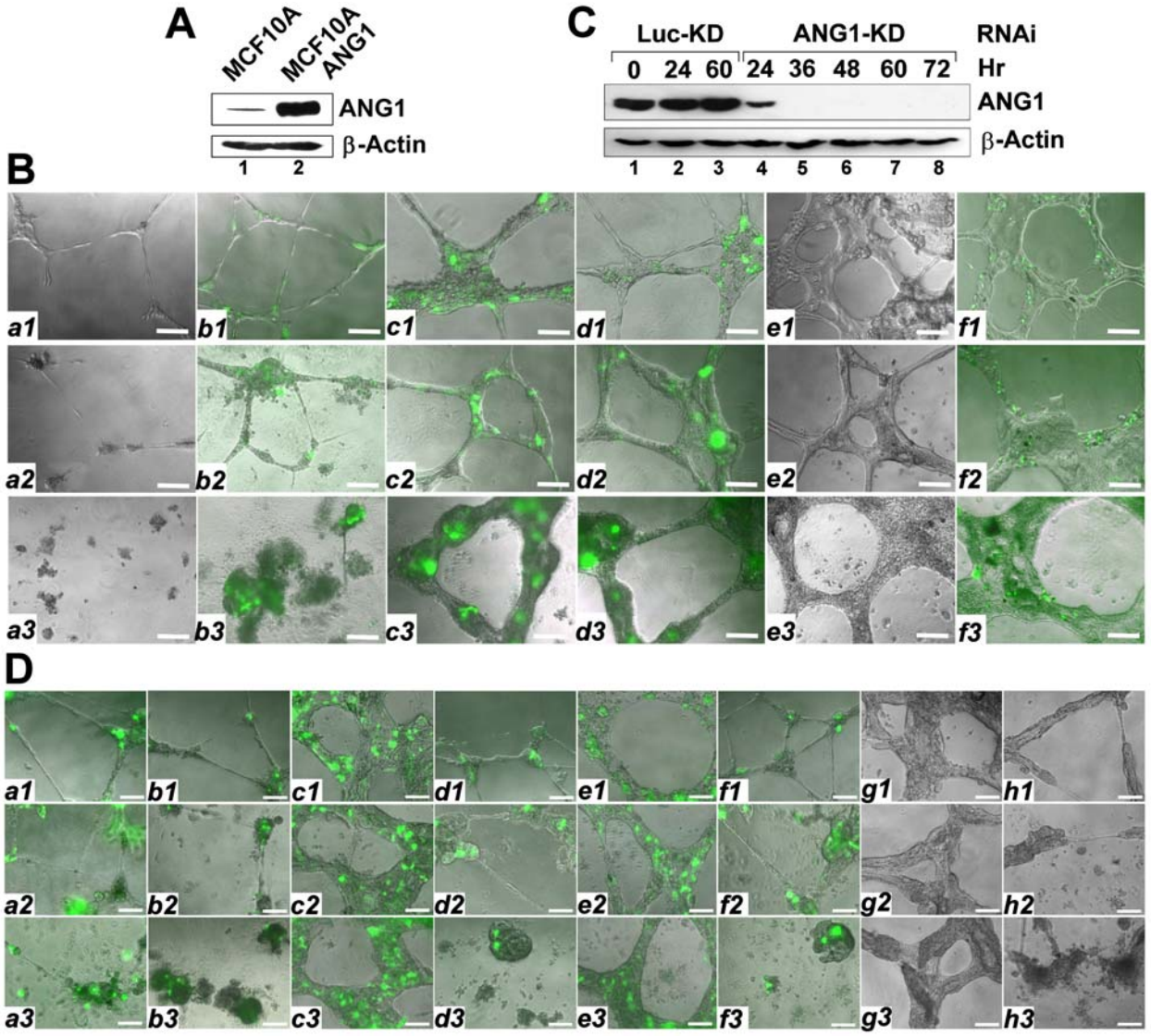
A
MCF10A
MCF10A ANG1
ANG1
β-Actin
1 2
C
Luc-KD
ANG1-KD
RNAi
0 24 60 24 36 48 60 72
Hr
ANG1
β-Actin
1 2 3 4 5 6 7 8
B
a1 b1 c1 d1 e1 f1
a2 b2 c2 d2 e2 f2
a3 b3 c3 d3 e3 f3
D
a1 b1 c1 d1 e1 f1 g1 h1
a2 b2 c2 d2 e2 f2 g2 h2
a3 b3 c3 d3 e3 f3 g3 h3

Figure 6.

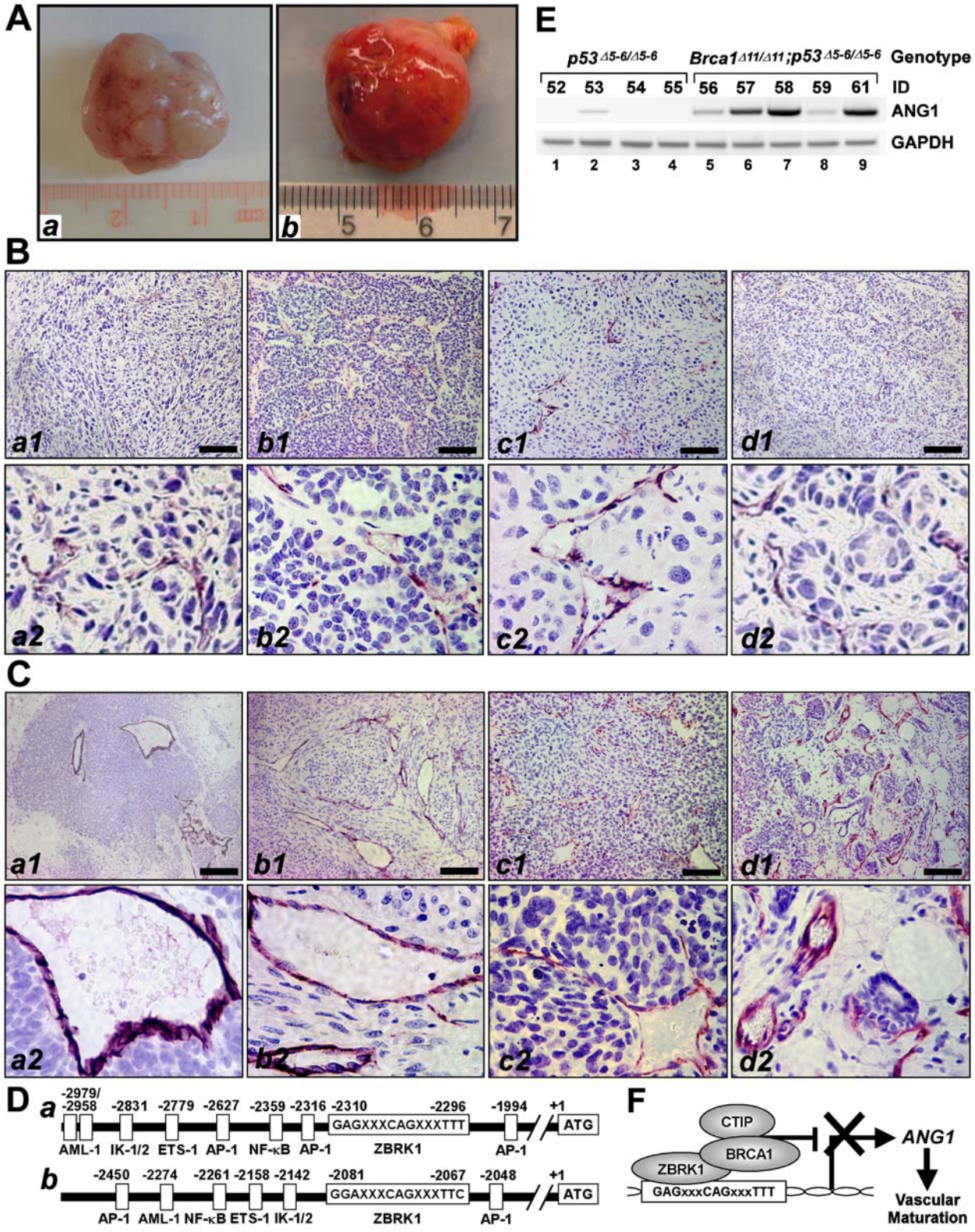
A
a
b
E
p53Δ5-6/Δ5-6
Brca1Δ11/Δ11;p53Δ5-6/Δ5-6
Genotype
52 53 54 55 56 57 58 59 61
ID
ANG1
GAPDH
1 2 3 4 5 6 7 8 9
B
a1 b1 c1 d1
a2 b2 c2 d2
C
a1 b1 c1 d1
a2 b2 c2 d2
D
a
-2979/ -2958 -2831 -2779 -2627 -2359 -2316 -2310 -2296 -1994 +1
GAGXXXCAGXXXTTT
ATG
AML-1 IK-1/2 ETS-1 AP-1 NF-κB AP-1 ZBRK1 AP-1
b
-2450 -2274 -2261 -2158 -2142 -2081 -2067 -2048 +1
GGAXXXCAGXXXTTC
ATG
AP-1 AML-1 NF-κB ETS-1 IK-1/2 ZBRK1 AP-1
F
CTIP
BRCA1
ZBRK1
GAGxxxCAGxxxTTT
ANG1
Vascular Maturation

Supplementary Table

Table S1. Primer sequences

Usage	Designation	F/R	Sequence
RT-PCR	α-Tubulin	F	5'-TGA CCT GAC AGA ATT CCA GAC CA-3'
		R	5'-GCA TTG ACA TCT TTG GGA ACC AC-3'
	ANG1	F	5'-GGA AGT CTA GAT TTC CAA AGA GGC-3'
		R	5'-CTT TAT CCC ATT CAG TTT TCC ATG-3'
	mANG1	F	5'-GGC ACG GAA GGC AAG CGC TG-3'
		R	5'-CAA GCA TGG TGG CCG TGT GG-3'
	β-Actin	F	5'-CCCAAGGCCAACCGCGAGAAG-3'
		R	5'-TCTTCATTGTGCTGGGTGCCA-3'
	BRCA1	F	5'-GAA GAA ACC ACC AAG GTC CA-'3
		R	5'-ATG GAA GCC ATT GTC CTC TG-3'
	CtIP	F	5'-AAG CAA GTA GAA GTG TGG AGC AT-3'
		R	5'-TCA GCT GCT TGA TGC TGT TGA TCA-3'
	FGF2	F	5'-AAG ATG GTA GCA CTA GTC-3'
		R	5'-GCA GAT TTG GTC ACT ACC-3'
	mGAPDH	F	5'-CAT TGA CCT TCA CTA CAT GGT-3'
		R	5'-ACC CTT CAA GTG AGC CCC AG-3'
	HMGA2	F	5'-CGA AAG GTG CTG GGC AGC TCC GG-3'
		R	5'-GAA GAA ACC ACC AAG GTC CA-3'
	LIMK1	F	5'-CTT CTC CTC AGG GCC AGG-3'
		R	5'-AGG GGC TGT TTG GTC AGC-3'
	RFC1	F	5'-CAA TAA TGA GCC TGG GAG-3'
		R	5'-GAC CAC TGC ATG AAA TCC-3'
	ZBRK1	F	5'-CCGTGGACAATTGAAGATGG-3'
		R	5'-TAAGTGACGTGTGTACTACGAAGAGAT-3'
Mutagenesis	BRCA1 (C61G)[1]	F	5'-GGG CCT TCA CAG **G**GT CCT TTA TGT AAG-3'
		R	5'-CTT ACA TAA AGG AC**C** CTG TGA AGG CCC-3'
	BRCA1 (Q356R)[1]	F	5'-GAA TGG AAT AAG C**G**G AAA CTG CCA TGC-3'
		R	5'-GCA TGG CAG TTT C**C**G CTT ATT CCA TTC-3'
	BRCA1 (M1775R)[1]	F	5'-GCC CTT CAC CAA CA**G** GCC CAC AGA TCA AC-3'
		R	5'-GTT GAT CTG TGG GC**C** TGT TGG TGA AGG GC -3'
	BRCA1 (RM)[1]	F	5'-GTA TGG GCT AC**C** G**G**A A**TA** G**G**G CCA AAA GAC TTC-3'
		R	5'-GAA GTC TTT TGG C**C**C **TA**T T**C**C **G**GT AGC CCA TAC-3'
	CtIP (S327A)[1]	F	5'-CTC GAG TGT CA**G** CTC CTG TAT TTG-3'
		R	5'-CAA ATA CAG GAG **C**TG ACA CTC GAG-3'
	CtIP (RM)[1]	F	5'-GTA TAG ATC CGG GAG C**T**G AC**T** T**G**T CTC AGT ATA AAA TGG-3'
		R	5'-CCA TTT TAT ACT GAG A**C**A **A**GT C**A**G CTC CCG GAT CTA TAC-3'
Reporter Mutagenesis	C1[2]	F	5'-GAG TCA ATT CTG CAC ATC CTT CTC GAG AGA AAC CTC ACC ACT CAT CCA-3'
		R	5'-TGG ATG AGT GGT GAG GTT TCT CTC GAG AAG GAT GTG CAG AAT TGA CTC-3'
	C2[2]	F	5'-AGA AAC CTC ACC ACT CAT CCA CTC GAG TTG CCT GAG TTC ACA TAC TGG-3'
		R	5'-CCA GTA TGT GAA CTC AGG CAA CTC GAG TGG ATG AGT GGT GAG GTT TCT-3'
	C3[2]	F	5'-GAG TCA ATT CTG CAC ATC CTT CTC GAG TTG CCT GAG TTC ACA TAC TGG-3'
		R	5'-CCA GTA TGT GAA CTC AGG CAA CTC GAG AAG GAT GTG CAG AAT TGA CTC-3'
	C-mt-Z[1]	F	5'-ACA CAC GTG G**TT** GA**T** **TT**G ATT TTT AAC AGT CTC-3'
		R	5'-GAG ACT GTT AAA AAT C**AA** **A**TC **AA**C CAC GTG TGT-3'
	3P-26-(wt/mt)-Z[2,3]	F	5'-GCT CTA GAA CAC AAC AGT GTT GCT GTT GC-3'
		R	5'-CCG CTC GAG CTA AGA TCA CGG ATA TCA TCC-3'
ChIP	ANG1 (-2400/-2100)	F	5'-TCC CTC AGG AAA TTG TGC ATT CCT GC-3'
		R	5'-CTA TGC ACA GCC ACA AAG ATG AAG TGC-3'
Retrovirus	ANG1 cDNA (-281/+1660)[4]	F	5'-GAA AGG ATC CAG TTT TGC GAG AGG CAC GGA A-3'
		R	5'-CCT TGG ATC CTT CAC ATA ACT ACC ACT TAT TGC-3'

[1]Mutation site shown underlined in bold.
[2]Incorporated *Xho*I restriction site shown underlined.
[3]Incorporated *Xba*I restriction site shown underlined.
[4]Incorporated *Bam*HI restriction site shown underlined.

Supplementary figure

S1. RT-PCR analysis of genes co-suppressed by BRCA1 and CtIP in 3-D cultured MCF10A cells

A: RT-PCR confirmation of several genes commonly upregulated in BRCA1- and CtIP-KD MCF10A cells by microarray analysis (Table 1). a. ANG1, b. HMGA2, c. FGF2, d. RFC1, and e. LIMK1. α-tubulin was used as the internal control. Respective primer sequences are shown in Table S1.

B: Relative expression levels of tested genes in BRCA1- and CtIP-KD MCF10A cells with respect to Luc-KD cells after normalization against α-tubulin.

Figure S1.

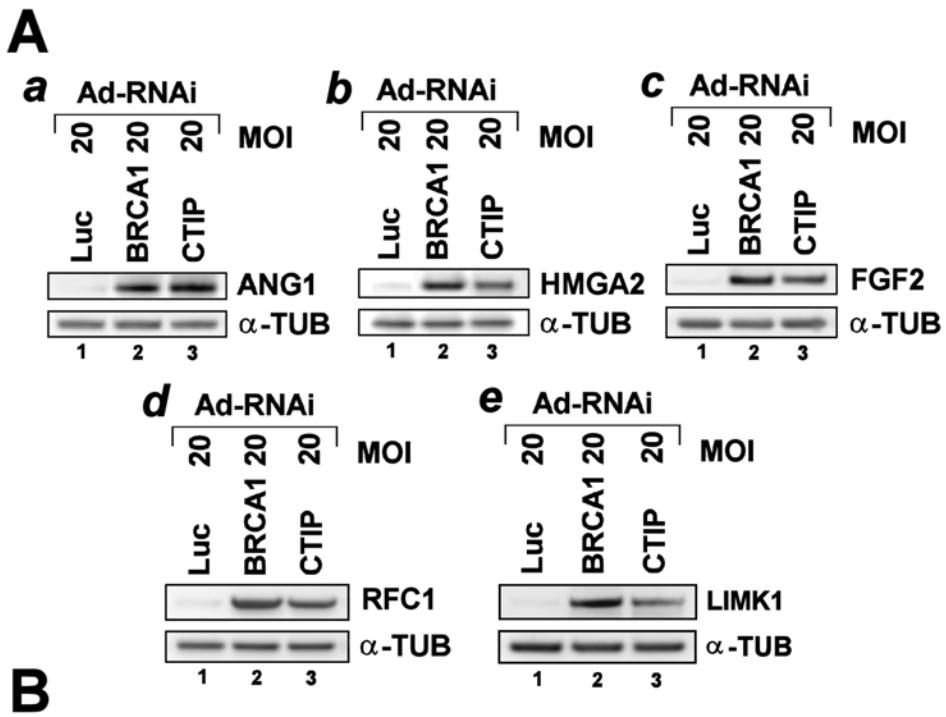

B

	ANG1	HMGA2	FGF2	RFC1	LIMK1
BRCA1-KD	+ 7.1	+ 6.9	+ 7.5	+ 7.3	+ 7.9
CTIP-KD	+ 8.0	+ 4.9	+ 4.7	+ 5.8	+ 4.1